FUNDAMENTALS OF A BULK-FLOW THEORY FOR TURBULENT LUBRICANT FILMS

PROEFSCHRIFT

TER VERKRIJGING VAN DE GRAAD VAN DOCTOR IN DE TECHNISCHE WETENSCHAPPEN AAN DE TECHNISCHE HOGESCHOOL DELFT, OP GEZAG VAN DE RECTOR MAGNIFICUS DR. IR. C. J. D. M. VERHAGEN, HOOGLERAAR IN DE AFDELING DER TECHNISCHE NATUURKUNDE, VOOR EEN COMMISSIE UIT DE SENAAT TE VERDEDIGEN OP WOENSDAG 1 JULI 1970 TE 14.00 UUR

DOOR

GILLES GERARDUS HIRS

werktuigkundig ingenieur

geboren te Haarlem

Dit proefschrift is goedgekeurd door de promotor
PROF. IR. H. BLOK.

CONTENTS: Page:

1. SCOPE

The purposes of this thesis on the turbulent lubricant film are:

(1) to give a brief outline and a general formulation of a newly developed semi-empirical theory, which the author prefers to name "bulk-flow theory";

(2) to examine to what extent experimental results published in literature agree with this theory;

(3) to investigate to what extent results of theories based on law-of-wall and mixing-length concept agree with the bulk-flow theory;

(4) to provide a sound theoretical basis for the selection and the design of bearings for liquid-sodium pumps and for other applications in which fluids of low kinematic viscosity are used as lubricants.

1. Doel

De doelstellingen van dit proefschrift over de turbulente smeerfilm zijn:

(1) een beschrijving en een algemene formulering van een door de auteur ontwikkelde, semi-empirische theorie;

(2) een onderzoek naar de mate van overeenstemming van aan de literatuur ontleende, experimentele resultaten met deze theorie;

(3) een onderzoek naar de mate van overeenstemming van de nieuwe theorie en theorieën gebaseerd op de wandwet en het menglengte principe;

(4) het verschaffen van een gezonde theoretische basis voor de keuze en het ontwerp van lagers voor vloeibaar-natrium pompen en voor andere toepassingen waarin media met lage kinematische viscositeit als smeermiddel gebruikt worden.

2. SUMMARY

A newly developed semi-empirical theory, the so-called "bulk-flow theory", allows pressures, flow rates and shear stresses in a turbulent lubricant film to be calculated, and, also, the further information, required for the design of turbulent lubricant film bearings, to be determined.

The author gave an outline of this theory and made a comprehensive study of literature on other theories and on experiments with turbulent flow in lubricant films o r comparable flow channels. Sufficient experimental data were found to warrant the conclusion that the bulk-flow theory is reliable for bearings with smooth, ungrooved, plane surfaces in the operational range covered by these data. Additional tests were shown to be needed on flows in between surfaces differing from the above-specified ones, viz.:

(1) curved surfaces
(2) non-equidistant surfaces
(3) rough surfaces
(4) grooved surfaces.

Additional tests could provide:

(a) a clearer insight into the question to which extent the bulk-flow theory is valid with the above-described surfaces
(b) fitted, more widely applicable, values for the empirical constants to be substituted in the bulk-flow theory.

Apart from this, such an investigation makes it possible to design more efficient bearings. For instance, it would appear possible to increase the load-carrying capacity and decrease energy consumption by giving part of one surface, or of both surfaces, a rough instead of a smooth finish or by giving part of one surface a pattern of shallow grooves.

It should be noted that it is of limited importance to make more tests with bearing surfaces of types (1) and (2) above. At least estimates of load-carrying capacity and energy consumption of bearings with the usual small clearances, based on existing theory, have proved to be less than 20 per cent too low.

From the comparison with results obtained from theories based on the law-of-wall and on the mixing-length concept, the newly developed bulk-flow theory emerges as the more reliable one in a greater range. This is due to the fact that physical models underlying the former two theories have a limited range of applicability. In the bulk-flow theory, however, no use is made of any physical model whatsoever for the turbulence mechanism. Instead of a model, a correlational observation was utilized in developing and fitting the present theory. That is, it was observed that there is a correlation between wall-shear stress, mean or bulk-flow velocity, film thickness, density, viscosity, and that this correlation is only weakly dependent on the nature of the flow in the lubricant film; whether this is "pressure flow", under the influence of a pressure gradient, or "drag flow" due to sliding of a surface, or any combination of these two basic types of flow. Further, the mean flow velocity in the most general type of flow, and relative to a bearing surface, could be conceived to be attributable to a representative pressure gradient. This representative gradient is defined as the sum of the real pressure gradient which accounts for the real pressure flow component and a fictitious pressure gradient which accounts for the other flow component: the drag-flow component. Thus, for any turbulent film two equations between representative pressure gradient and mean flow velocity can be established, one for either bearing surface. These two equations suffice for determining pressures, flow rates and shear stresses in turbulent lubricant films.

The last part of the thesis is devoted to design directives for turbulent self-acting fluid film bearings. It proves to be a major benefit of the bulk-flow theory that such directives can be cast into an extremely simple and concise form.

2. SAMENVATTING

Met een nieuwe, semi-empirische theorie, die "bulk-flow theory" gedoopt werd, is het mogelijk om drukken, stromen en schuifspanningen in een turbulente smeerfilm te bepalen en ook om de verdere informatie, die voor het ontwerpen van lagers met een turbulente smeerfilm nodig is, te verkrijgen.

De auteur gaf een beschrijving van deze theorie en maakte een literatuurstudie over andere theorieën en over experimenten aan turbulente stroming in smeerfilmen of vergelijkbare stromingskanalen. Voldoende experimentele gegevens werden gevonden om te kunnen concluderen dat de nieuwe theorie bruikbaar is voor lagers met gladde, ongegroefde, vlakke loopvlakken.

Aangetoond werd dat meer proeven nodig zijn met stroming tussen loopvlakken met de volgende, van het bovenstaande afwijkende, eigenschappen:

1 gekromd
2 niet-parallel
3 ruw
4 gegroefd.

Zulke aanvullende proeven zouden leiden tot:

a) uitbreiding van inzicht in de mate van geldigheid van de nieuwe theorie voor deze loopvlakken
b) aangepaste, meer algemeen geldende waarden voor de empirische constanten die in de nieuwe theorie toegepast moeten worden.

Bovendien zullen aanvullende proeven het mogelijk maken betere lagers te ontwerpen. Zo is het bijvoorbeeld mogelijk het draagvermogen te verhogen en het energieverbruik te verlagen van lagers met geheel of gedeeltelijk ruwe loopvlakken of van lagers waarvan één der loopvlakken voorzien is van een patroon van ondiepe groeven.

Het belang van aanvullende proeven met loopvlakken van de typen (1) en (2) is beperkt. Schattingen van draagvermogen en energieverbruik van lagers met de gebruikelijke kleine spelingen, gebaseerd op bestaande theoretische gegevens, bleken minder dan 20 procent te laag te zijn.

Uit een vergelijking met theorieën gebaseerd op de wandwet en

het menglengte-principe, bleek de nieuwe theorie over een groter gebied de meest betrouwbare te zijn. Dit is te danken aan het feit dat physische modellen, die de basis vormen van de eerste twee theorieën, slechts in een beperkt gebied geldig zijn. In de nieuwe theorie, daarentegen, wordt *géén* model van het turbulentie-mechanisme toegepast. In plaats van een physisch model werd een correlerende waarneming gebruikt voor het ontwikkelen en aanpassen van de theorie. Het bleek namelijk dat er een correlatie van wandschuifspanning, gemiddelde stroomsnelheid, filmdikte, dichtheid en viscositeit bestaat en dat deze correlatie slechts zwak afhankelijk is van het type stroming in de smeerfilm ("drukstroming" onder invloed van een drukgradient, "sleurstroming" ten gevolge van het glijden van een loopvlak of een combinatie van deze twee basistypen). De gemiddelde stroomsnelheid ten opzichte van een loopvlak kan dan toegeschreven worden aan een representatieve drukgradient. Deze representatieve drukgradient is per definitie de som van de werkelijke drukgradient, die verbonden is met de drukstromingscomponent en een fictieve drukgradient, die verbonden is met de andere stromingscomponent: sleurstromingscomponent. Voor elke turbulente smeerfilm kunnen dus twee vergelijkingen tussen een representatieve drukgradient en een gemiddelde stroomsnelheid opgesteld worden: één vergelijking voor elk loopvlak. Deze twee vergelijkingen zijn voldoende voor het bepalen van drukken, stromen en schuifspanningen in turbulente smeerfilmen.

Het laatste deel van dit proefschrift is gewijd aan een ontwerpmethode voor turbulente, zelfwerkende glijlagers. Eén van de belangrijkste voordelen van de nieuwe theorie is het feit dat deze methode uiterst eenvoudig en beknopt blijkt te kunnen zijn.

3. INTRODUCTION

The bulk-flow theory for turbulent lubricant films is useful for applications in which process fluids with low kinematic viscosities are used as lubricants. However, the major incentive to develop the theory was found in the rather hostile conditions prevailing in large sodium pumps for nuclear breeder-reactors.

When pumping high-temperature liquid sodium with a centrifugal pump, it is not possible to lubricate all the bearings with some conventional, high viscosity lubricant. At least one bearing (the one nearest the pump impeller) cannot very well be lubricated otherwise than with the process liquid itself, i.e. sodium. This means that here there is no real choice between the two main types of bearings: rolling-element bearing or fluid-film bearing. Indeed, the former must immediately be discarded, the concentrated contact between counterformal surfaces and the resulting high contact stresses having proved disastrous when high temperature, liquid sodium is used as a lubricant. This appears e.g. from tests with various combinations of surfaces, immersed in sodium. With fluid-film bearings, however, the surfaces are conformal and contact stresses are lower. Besides, with fluid-film bearings it is possible, due to the conformity of the surfaces, to reduce contact between the surfaces to a minimum by providing for a continuous lubricant film which is much thicker than the differential heat distortion, and than the composite height of the irregularities due to machining, etc.

In this report we are not concerned with the selection of surface materials for these fluid film bearings but we will focus our attention on the lubricant film between the surfaces. More particularly, we will consider the pressure build-up and flow in such a lubricant film, for, therefrom, the load-carrying capacity, leakage, and energy consumption for bearings with lubricant films can be derived. Especially in the case of lubrication with sodium, it is necessary to pay meticulous attention to these factors since:

(1) when sodium is used as lubricant, the lubricant film will in general be turbulent whilst inertia effects other than those due to turbulence may also occur in the film and these effects make it difficult to predict the performance of these bearings with sufficient accuracy;

(2) in case of jamming or rapid wear of a bearing, pumps for liquid sodium require more expensive repair than pumps for other process liquids and/or pumps not lubricated with the process liquid but with a lubricating oil. In other words, sodium pumps require bearings of a highly dependable design but the available data do not suffice for making such a design.

It must be emphasized that a well designed bearing is not all by itself a guarantee for satisfactory operation of the pump as a whole. As an example of what may go wrong in a pump with a properly designed bearing we may mention axially asymmetrical heat distortion of the pump casing. When such a distortion occurs, the sodium-lubricated bearing, whether or not operating in conjunction with a second bearing, will have to bend the shaft in such a way that the surface of the former bearing may maintain its separation from the shaft surface by a lubricant film. Since the maximum hydrodynamically attainable force exerted on the shaft by externally pressurized bearings is proportional to the square of the shaft diameter whilst the bending force to be exerted by a bearing is proportional to the fourth power of the shaft diameter, it will be obvious that, if the other dimensions and operating conditions are held fixed, the diameter of the shaft should be selected as small as possible. Indeed, then the maximum axially asymmetrical heat distortion of the pump casing will affect the proper operation of the pump least adversely. Yet, when designing sodium pumps, the shaft diameter is usually chosen rather large in order to keep critical speeds above the normal speed range. The diameter could be made much smaller if the torque to be transmitted were the only factor of consideration. Therefore, sodium pumps should preferably be provided with thin shafts and flexure due to supercritical running should be reduced e.g. by a damper as was done by Voorhees (1967)[1].

It would be outside the scope of this report to discuss the entire design of a pump, and even the various designs of the bearing can only be briefly described, see Fig. 1.[2] With any of these designs it is in principle possible to achieve a lubricant film of acceptable minimum thickness in a sodium pump.

[1]) See List of References, p. 68. [2]) See page 17.

The bearing shown in Fig. 1a is the self-acting plain cylindrical bearing. It owes its load-carrying capacity to the pumping action in the bearing proper: due to the sliding of one of the surfaces, the lubricant is forced into a converging wedge-shaped slit, and this induces an increase in pressure if inertia effects in the flowing liquid are not dominant.[1])

The bearing of Fig. 1b is the self-acting bearing with a symmetrical groove pattern. This bearing owes its load-carrying capacity not only to the aforementioned wedge effect but also to the pumping action of the grooves. An advantage of this type of bearing is the greater stability towards disturbances of the equilibrium between the resultant of the forces set up in the lubricant film and the external force acting on the bearing."[2])

The self-acting tilting-pad bearing, Fig. 1c, has much lower load-carrying capacity than the bearings of Figs. 1a and 1b but its stability is very good."'[3])

Regarding the three self-acting bearings of Figs. 1a, 1b and 1c, it should be noted that for large sodium pumps it is very difficult, if not impossible, to provide for sufficient load-carrying capacity with the correspondingly large minimum film thickness to be aimed at. Fortunately, the excess pressure created by the pump impeller can also be used to increase the load-carrying capacity, i.e. by changing over from self-acting to externally pressurized bearings. Indeed, the pump itself may be utilized as the external pressure source for the latter type of bearings.

The bearing shown in Fig. 1d is an externally pressurized cylindrical bearing with external restrictions in the form of circumferential slots.""[4])The sketch shows that external restrictions are

') Numerous textbooks give information about this bearing when operating in a laminar regime. Smith and Fuller (1956), Duffin and Johnson (1966) and Ketola and Mc Hugh (1967) give information in the turbulent regime.

") For laminar operation see Hirs (1965) and for turbulent operation Chow and Vohr (1969).

"') For both laminar and turbulent operation see Orcutt (1967).

"") For laminar operation see numerous textbooks, for turbulent operation of a slightly modified bearing, see Roberts and Betts (1969).

indispensable for creating pressure differences along the circumference, i.e. for creating load-carrying capacity.

The bearing of Fig. 1e has locally recessed zones, the external restrictions being in the form of capillaries or orifices.[1]) Its load-carrying capacity is higher than that of the bearing of Fig. 1d, especially with larger width/diameter ratios.

A third type of externally pressurized bearing is shown in Fig. 1f; the left-hand side of the bearing is the high-pressure side. The main difference between this bearing and the two previous types is the absence of external restrictions and the presence of shallow axial grooves on the journal. It will be seen from Fig. 1f that, by virtue of these grooves, differences in pressure may be generated along the circumference of the shaft so that they will result in load-carrying capacity."[2]) The load-carrying capacity of this bearing proves to be approximately the same as that of the bearing of Fig. 1d. All three types of externally pressurized bearings show good stability of the equilibrium between the resultant of the forces created in the lubricant film and the external force. As compared with the other types, the bearing of Fig. 1e is at some disadvantage, due to the ineffectiveness of damping the deviations from the equilibrium position of the shaft relative to the bearing.

In this brief review of externally pressurized bearings the effect of the sliding of a surface on the turbulent operation of the bearing has so far been left out of consideration."'[3]) Especially with smaller radial clearances, the effect of sliding of a surface results in much poorer stability of the unrecessed bearing of Fig. 1d and in a decrease in load-carrying capacity of the recessed bearing of Fig. 1e. Both the stability and the load-carrying capacity of the bearing of Fig. 1f change but little due to the sliding of a surface. The only type of bearing known to the author in which both the external pressurization and the pumping effect due to the sliding of a surface

') See last footnote on page 14.

") For laminar operation see Hirs (1966).

"') Little has been published until now about this subject; Yamada's work (1962) is the main source from which the overall properties have been derived.

may strongly improve the load-carrying capacity as well as the stability is the one shown in Fig. 1g. For that reason, it seems justified to term the bearing of Fig. 1g a truly "hybrid" bearing.

Theoretical and experimental work is envisaged to take into account the turbulence and the other inertia effects occurring in the lubricant films in the various types of bearings of Fig. 1 when a low-viscosity fluid, such as sodium, is used. Such work would enable any type of bearing to be optimized for its maximum load-carrying capacity and/or stability. Also, one may then quantitatively compare the various bearing types of Fig. 1 with one another. Optimization of the bearing of Fig. 1g, which would probably emerge as the best design, would obviously be the most laborious piece of work.

Naturally, load-carrying capacity and stability are not the only factors that play a role in selecting the type of bearing. Simplicity of design, for instance, is probably most conspicuous in the bearing of Fig. 1a (which however is not practical in most applications), and in the bearings of Figs. 1d and 1f.

It is perhaps needless to say that optimization will not only result in the optimum design parameters giving the highest stability and/or the highest load-carrying capacity of these bearings, but also in the utmost reliability. This is due to the fact that insufficiently controllable deviations from the design parameters which, for instance through the workshop tolerances, will always occur in actual practice, will have less disastrous consequences according as these design parameters correspond better with the optimum design parameters. In fact, not only is an optimum worth aiming at all for itself, but also for the valuable feature that in its vicinity the sensitivity of performance toward deviations from the optimum naturally uses to be much smaller than somewhere far off the optimum.

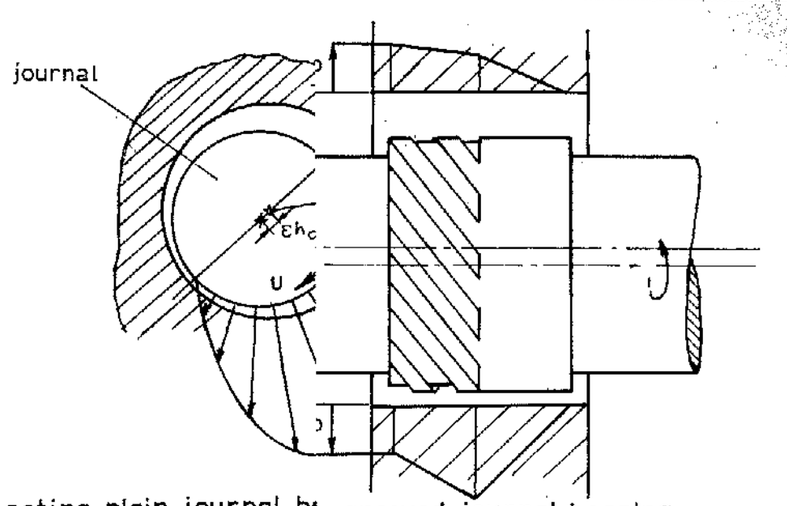

g

Self-acting, plain journal be grooved, journal bearing

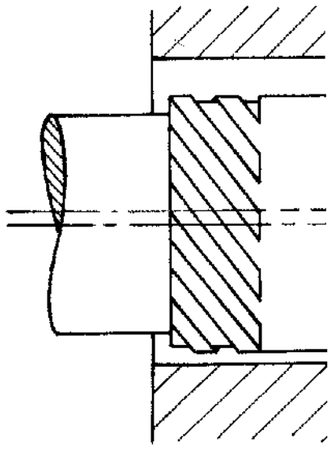

Self-acting, partly grooved

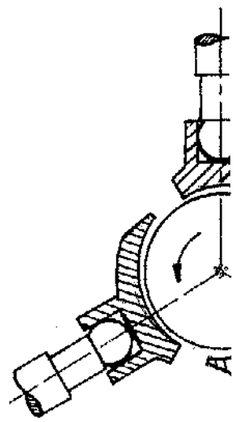

Self acting, tilting pad journ

Fig. 1

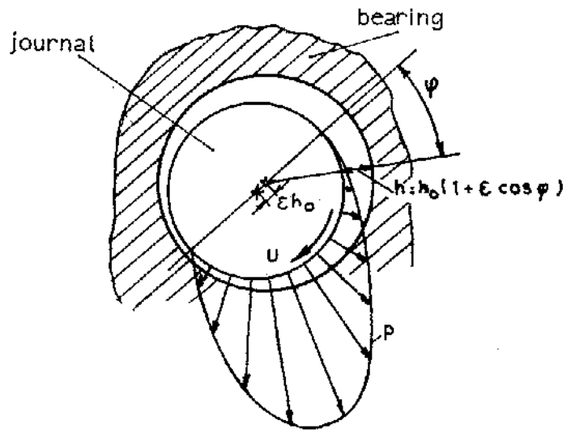

a

Self-acting, plain journal bearing

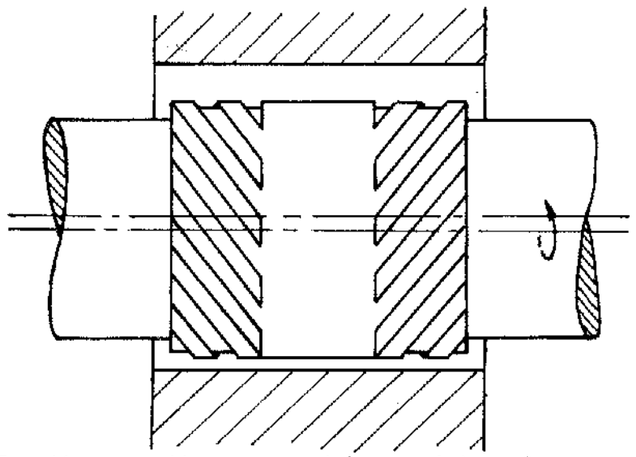

b

Self-acting, partly grooved journal bearing

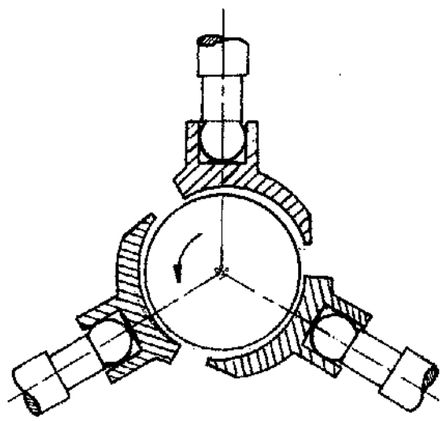

c

Self acting, tilting pad journal bearing

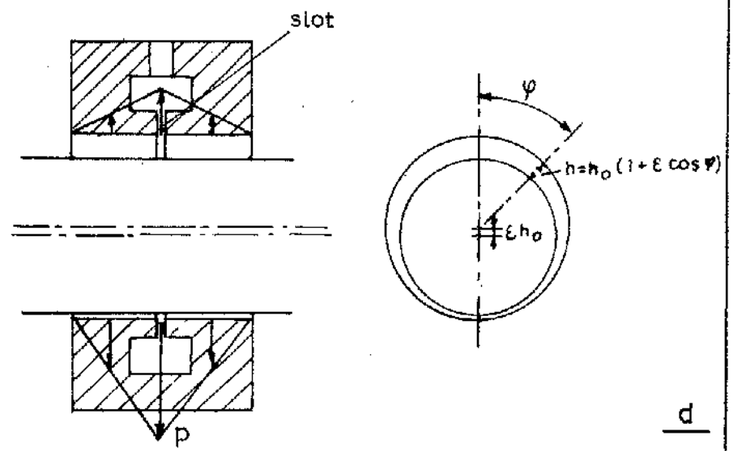

d

Externally pressurized, slotted journal bearing

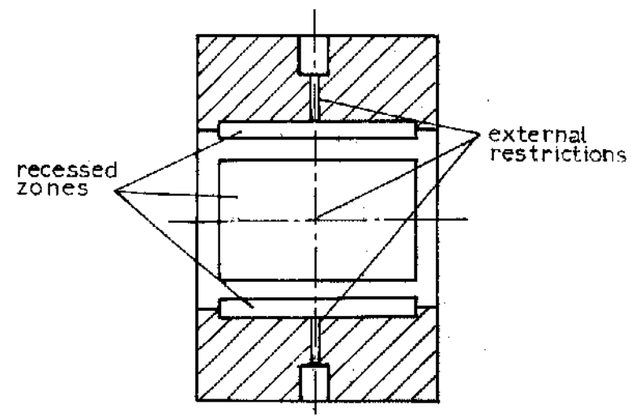

e

Externally pressurized, locally recessed journal bearing

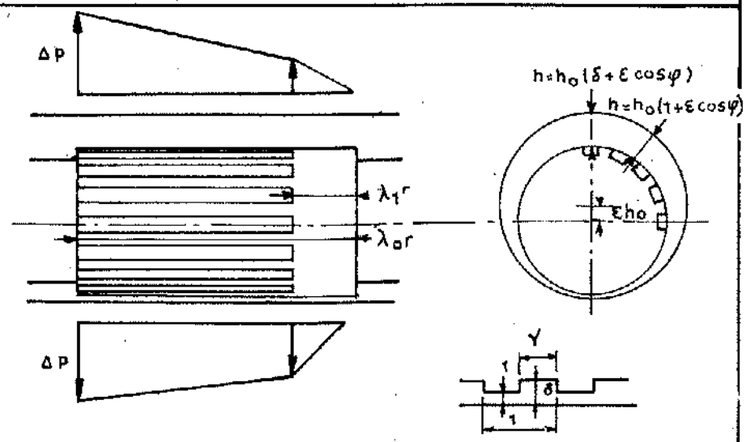

f

Externally pressurized, partly grooved journal bearing

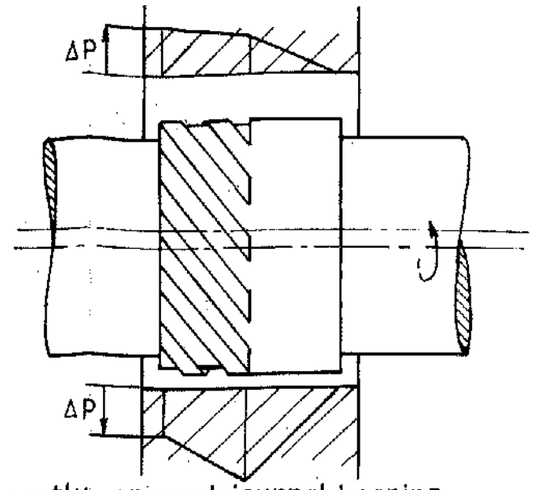

g

Hybrid, partly grooved, journal bearing

Fig. 1

4. DIFFERENT THEORIES OF THE TURBULENT LUBRICANT FILM

4.1. Purely fundamental theory.

It is more difficult to predict pressure build-up and flow in a turbulent lubricant film than in a laminar lubricant film since the Navier-Stokes equations, which are applicable to both types of lubricant film, cannot be sufficiently simplified in the case of the turbulent lubricant film to obtain equations with simple solutions.

Moreover, the existing and commonly used simplification method for turbulent flow, consisting in averaging the fluctuations in velocity of flow, pressure and density or combinations thereof, over an acceptably large period of time and an acceptably large area, results in a number of additional unknown factors in the equations. These unknown factors, especially the averages of products of flow velocity fluctuations, cannot yet be determined theoretically. One might try to measure them in lubricant films for a large number of cases and to use the experimental data for substituting into, and thus solving, the Navier-Stokes equations. Although sufficient experimental data are not yet available, this method has been shown to be promising, as is evidenced by the tests of Carper et al (1963), Laufer (1954) and Reihardt (1956) on flow under the influence of a pressure gradient in a channel of rectangular cross section, and of those of Burton (1967) on flow induced in the annulus between cylindrical surfaces by the sliding of one of these surfaces, in some cases even combined with a flow component under the influence of a pressure gradient. However, the measuring procedure concerned (hot-wire method) is very laborious and, moreover, it seems difficult (considering some remarks in the above-mentioned publications) to obtain reliable results.

Solving the Navier-Stokes equations with the aid of such experimental data is no doubt the most fundamental approach nowadays available for predicting the pressure build-up and flow in a turbulent lubricant film. However, the computational effort involved is extremely large. It is evident that this method does not rapidly yield results and that it is a rather complicated one for calculating the load-carrying capacity and leakage of turbulent bearings. Also in

view of the promising initial results obtained in a piece of fundamental research by Burton (1967), it is recommended to perform such investigations in a laboratory especially devoted to the fundamental aspects of turbulence as a general discipline. Such investigations would permit a critical judgement of the less fundamental theories discussed in the following paragraphs and of the bearing calculations there made or of those to be made in the future on the basis of these theories.

4.2. Mixing-length theory.

A prediction of pressure build-up and flow in a turbulent lubricant film is possible on the basis of a theory developed by Constantinescu (1969), and based on the classical mixing-length concept.

4.3. Law-of-wall theory.

This theory (adapted by Elrod and Ng (1967) to the turbulent lubricant film) is based on the hypothesis that there is a universal shape of the time-averaged and suitably normalized portions of the flow-velocity profile that are in the vicinity of the surfaces bounding the lubricant film.

The hypotheses of both theories permit to confine oneself to a limited number of measurements of flow velocity profiles, to derive therefrom certain hypothetical constants, and then to calculate flow velocity profiles for all combinations of the two components of flow, that is, "pressure flow" under influence of a pressure gradient and "drag flow" due to the sliding of a surface. A shortcoming of both theories is the fact that, as appears e.g. from Burton's experiments, the hypotheses are, not sufficiently applicable to all points of the lubricant film and to all operating conditions. Yet, Burton (1967) concludes that both calculating methods eventually yield flow velocity profiles which do not depart too much from the actual ones. It may be added here that experiments by Orcutt (1967) and others with a tilting-pad bearing (Fig. 1c) show that the load-carrying capacity can be accurately predicted by the law-of-wall theory. Judging from Constantinescu's findings (1967 and 1969), reasonable agreement with experimental results can probably also be achieved by using the mixing-length theory.

Why then is it not to be recommended to base further calculations of bearings as shown in Fig. 1 on one of these two theories? The reasons are the following:

(a) with both the mixing-length theory and the law-of-wall theory, flow velocity profiles must be determined for a sufficient number of combinations of the drag flow and pressure flow components; this determination will require much computation; the resulting profiles can only be integrated numerically to yield bulk-flow velocities;

(b) empirical constants necessary for predicting these profiles must be fitted to measurements of actual flow velocity profiles;

(c) so far these empirical constants are known only for smooth and flat surfaces and for flow without inertia effects; hence, so as to enable extensions to computational work, much supplementary experimental work would have to be done in order to further develop the two methods concerned;

(d) computations based on these two theories have so far been made only for self-acting bearings;

(e) in the regime of low Reynolds numbers (1000-10,000), which is important for bearings, the two theories give results that deviate from experiments because, as will be shown in chapter 7, the underlying physical models are not valid in this regime.

4.4. Mid-channel velocity theory.

Burton (1967) was aware of the above-mentioned shortcomings and arrived at a much simpler theoretical approach by interrelating all basic characteristics of a lubricant film, such as pressure gradient, sliding velocity of a surface, and shear stresses at either surface, to a characteristic velocity of flow in the lubricant film, the "mid-channel velocity", defined as the one at the midplane between the two surfaces. He succeeded in doing this by using simplified time-averaged, flow-velocity profiles. This theory is indeed so simple that inertia effects in the flow can readily be included in the calculations. However, computations based on this method have again been confined to very simple types of self-acting bearings and an extension

of this theory to externally pressurized and hybrid bearings would appear extremely difficult.

4.5. Bulk-flow theory.

All of the three abovementioned theories are based on information obtained from experiments regarding:

(a) fluctuating velocity components due to turbulence;
or
(b) velocity profiles so time-averaged as to eliminate fluctuating velocity components.

It has been sufficiently demonstrated in the foregoing that this approach is subject to difficulties in measuring velocities of flow and in processing the experimental data. Therefore, the author has made an attempt at a sufficiently accurate description of pressure build-up and flow in a lubricant film that is based on correlational data about bulk-flow relative to each of the two bearing surfaces. It proves indeed possible to develop a theory on the basis of such information and to calculate quite a variety of bearing types, self acting, hybrid as well as externally pressurized ones.

This bulk-flow theory is based on an analogy between turbulent flow under the influence of a pressure gradient and the one due to the sliding of a surface. It had been found already by Davies and White (1929) and Couette (1890), respectively, that in either type of turbulent flow the wall shear stress depends on density, viscosity mean flow velocity with respect to the particular surface for which the shear stress is considered, and thickness of the fluid film. Combining their findings, it can be shown that in either type the representation of this dependency requires, as a minimum, two dimensionless groups, e.g. a friction factor and a Reynolds number. When plotting these dimensionless groups against each other in graphs, it is striking, that in the turbulent regime the curve representing experiments for pressure flow is remarkably close to that representing drag flow.[1])

Thus, it can be concluded that the dependency of the two dimensionless groups and, thus, the dependency of wall shear stress on density, viscosity, mean flow velocity with respect to the surface con-

[1]) Burton (1967) has found an even closer agreement between the two flow types when using mid-channel velocity instead of mean flow velocity.

cerned and film thickness is fairly insensitive toward the type of flow in the lubricant film. The author has found evidence that these dependencies are also insensitive to fairly general kinds of combinations of the two flow components such as mutually perpendicular flows, one being a pressure flow and the other a drag flow. It is the insensitivity of wall shear stress to the type of flow that has led the author to a treatment of flow in lubricant films that is made unifying in that a pressure gradient is introduced as a criterion not only for pressure flow but also for drag flow, the latter pressure-gradient being, of course, a fictitious one. Thus, the actual rate of flow in a lubricant film with respect to each one of the surfaces can be treated, as if it consists of two superimposed flow components, one under the influence of the actual pressure gradient and the other under the influence of the fictitious pressure gradient. Through this treatment flow in lubricant films with sliding surfaces can be treated in a manner comparable to that for flow in lubricant films with stationary surfaces. Moreover, the experimental information needed may be confined to the dependency of friction factor on Reynolds number for real pressure flow, i.e. the one under the influence of an actual pressure gradient.

This thesis will also deal with a method of incorporating, in the present theory, inertia effects in the flow, other than those inherent in turbulence. In addition, it will be demonstrated that the effects of roughness and grooving of surfaces on the film interposed can be accounted for in this theory in a most simple way.

5. OUTLINE OF THE BULK-FLOW THEORY

The main characteristic of the bulk-flow theory of the turbulent lubricant film is the fact that it does not make use of any explicit information, nor of any model, on:

(1) fluctuations of local velocities of flow due to turbulence;

(2) the shape of flow velocity profiles from which fluctuating components have been eliminated throug averaging.

In this theory only the rate of bulk-flow relative to a surface or wall and the corresponding shear stress at that surface or wall under a given set of conditions of turbulent flow are considered and correlated.

The author's approach is essentially a logical extension to basic work done by Blasius (1913) on turbulent "pressure flow", i.e. under the influence of a pressure gradient, in a pipe, by Davies and White (1929) on a similar flow between two stationary parallel surfaces, by Couette (1890) on turbulent "drag flow" between two concentric cylindrical surfaces due to the sliding of one surface, and by investigators who later have added experimental results of related types of flows to the previous pioneer work. Briefly summarized, the present theory is primarily based on the empirical finding that the relationship between wall-shear stress and mean velocity of flow relative to the wall at which the shear stress is exerted can be expressed by a formula common to "pressure flow" and "drag flow" and also to any combination of these two basic types of flow:

$$\frac{\tau}{\frac{1}{2}\rho u_m^2} = n \left(\frac{\rho u_m h}{\eta}\right)^m \qquad (1a)^{1)}$$

where

[1] Other more concise and more general expressions have been developed. The present two dimensionless groups and the power law form have been chosen for historical and practical reasons. Indeed, Blasius published his experimental results by assigning values to n and m, a form of presenting data still most widely used.

τ = wall-shear stress

ρ = density of flowing fluid

η = dynamic viscosity of flowing fluid

u_m = mean velocity of flow relative to wall or surface at which shear stress τ is exerted

h = film thickness.

n and m = empirical numerical constants to be fitted to the available experimental results throughout the range covered

$\frac{\rho u_m h}{\eta}$ = Re Reynolds number, [1])

and

$\frac{\tau}{\frac{1}{2}\rho u_m^2}$ = friction factor

In the above formula, the friction factor depends only weakly on the Reynolds number. In all experimental results available this property is evident from the fact that the m-values come close to zero, falling in the range $-0.5 < m < 0$.

Values for n and m fitted to individual experiments will be given in chapter 6. These values will be shown to depend, albeit rather weakly, on:

(1) the roughness of the surfaces;

(2) the curvature of the surfaces;

(3) the question of whether or not the Reynolds number is greater than about 100,000;

(4) the influence of inertia effects other than those inherent in turbulence in the flow;

(5) the types of flow:

  (a) "pressure flow" under the influence of a pressure gradient

  (b) "drag flow" due to the sliding of a surface

  (c) the nature of the combination, if any, of both types (a) and (b) as components of flow, which in the most general combination may even have non-parallel directions.

(6) the rates of change of all quantities indicated in formula (1a); these quantities may vary moderately in a lubricant film without violating the applicability of formula (1a)

[1]) In many publications, symbol Re is replaced by R or N_R.

It is stressed that mean flow velocity u_m in formula (1a) is taken relative to the surface at which shear stress τ is exerted, whilst bearings have two surfaces at which stresses are exerted. At most one surface can be considered to be stationary, the other being free to slide. Therefore, more specialized formulae than (1a) are determined for either surface. In the convention that is typical of the bulk-flow theory, the frame of reference is attached to the stationary surface and, accordingly, both the mean flow velocity u_m in the film and the sliding speed U of the sliding surface are to be taken with respect to the frame of reference. An extra limiting condition at this stage of the development of the theory is that u_m and U are in parallel directions. So, two formulae can now be derived, viz., one for the stationary surface:

$$\frac{\tau_a}{\frac{1}{2}\rho u_m^2} = n \left(\frac{\rho u_m h}{\eta}\right)^m \qquad (1b)\ ^{"})$$

and the other for the sliding surface:

$$\frac{\tau_b}{\frac{1}{2}\rho (u_m - U)^2} = n \left\{\frac{\rho (u_m - U) h}{\eta}\right\}^m \qquad (1c)\ ^{"})$$

in which the wall shear stresses are characterized by subscripts a and b, respectively. Formula (1b) gives shear stress τ_a and mean flow velocity with respect to the stationary surface (u_m). Formula (1c) gives shear stress τ_b and mean flow velocity with respect to the sliding surface (u_m-U).

For our further outline of the bulk-flow theory it is useful to realize that similarity and consistency of the two types of flow (flow under the influence of a pressure gradient and flow due to the sliding of a surface) is not only evident from the fact that the two relationships for τ have a similar form but also from the fact that the two values for n, n_o and n_1, as well as the two values for m, m_o and m_1, differ but little. This consistency can be further clarified by considering the two limiting cases represented by formulae (1b) and (1c) as far as the type of flow is concerned:

") For physical reasons, the m th power must treated as if it were an odd number in order to make the functional relationship odd.

(a) pressure flow, i.e. flow solely under the influence of a pressure gradient (Fig. 2a):

$$\frac{\tau_o}{\frac{1}{2}\rho u_{m_o}^2} = n_o \left(\frac{\rho u_{m_o} h}{\eta}\right)^{m_o} \qquad (2)$$

which can be derived from formulae (1b) and (1c) by inserting U=0 and which yields equal shear stresses on the two surfaces: $\tau_a = \tau_b = \tau_o$

(b) drag flow, i.e. flow solely due to the sliding of a surface (Fig. 2b):

$$\frac{\tau_1}{\frac{1}{2}\rho u_{m_1}^2} = n_1 \left(\frac{\rho u_{m_1} h}{\eta}\right)^{m_1} \qquad (3)$$

which is also based on (1b) and (1c) and in which $u_{m_1} = \frac{1}{2} U$ for the stationary surface and $u_{m_1} = -\frac{1}{2} U$ for the sliding surface and which should be taken to yield equal but opposite shear stresses on the two surfaces: $\tau_a = -\tau_b = \tau_1$.

Judging from experimental data to be described in chapter 6, the two extreme cases represented by formulae (2) and (3), as specializations of the general formulae (1b) and (1c), respectively, do show the abovementioned characteristic, viz., that the value of n_o/n_1 as well as that of m_o/m_1 comes close to unity. This similarity of formulae (2) and (3) exists despite the differences in shear stress distribution between:

(1) pressure flow, see Fig. 2a, with an inversely symmetrical shear stress distribution varying linearly with height z;

(2) drag flow due to the sliding of a surface, see Fig. 2b, with a constant shear stress distribution, independent of height z.

The absence of any appreciable influence of the shape of the shear stress profile across the film on the values of constants n and m in the formulae (2) and (3) for the turbulent regime leads to the following conclusions:

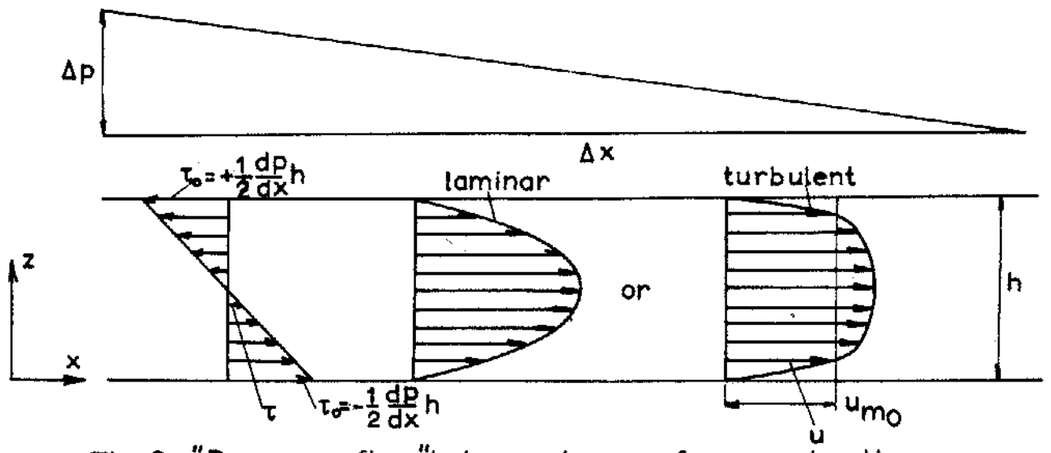

Fig. 2a "Pressure flow" between two surfaces under the influence of a pressure gradient.

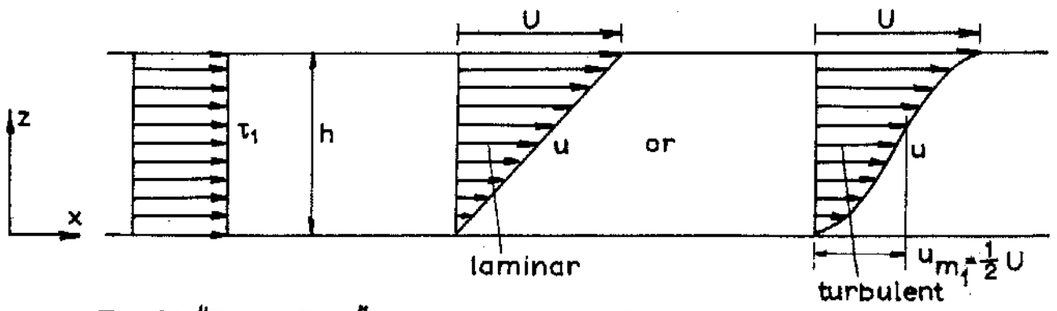

Fig. 2b "Drag flow" between two surfaces due to the sliding of one of them.

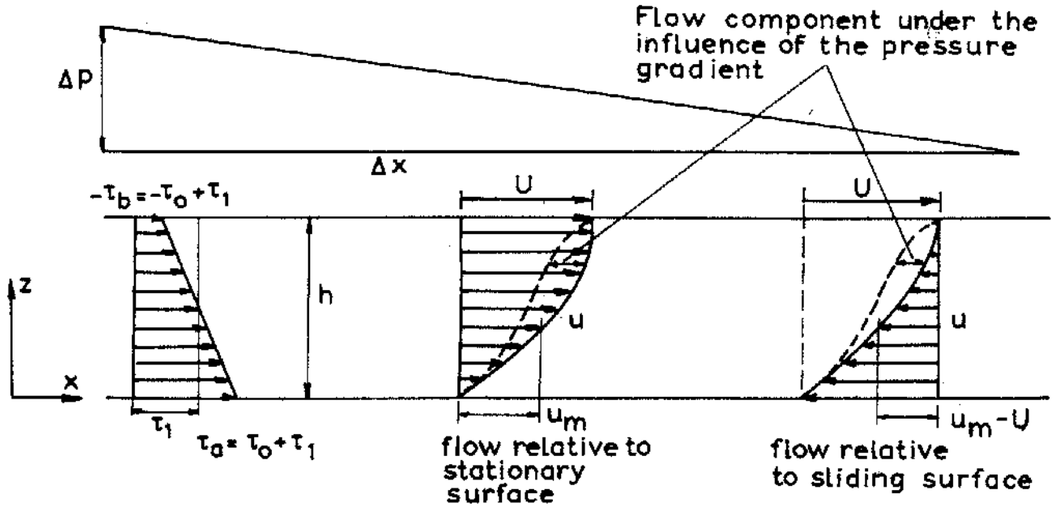

Fig. 2c "Turbulent flow" between two surfaces under the influence of a pressure gradient and due to the sliding of a surface.

1. The relationship between the shear stress at a surface and the mean velocity of flow relative to that surface depends but little on the type of flow, i.e. being valid to a reasonable approximation for pressure flow, drag flow, as well as for combinations of both.

2. For a first approximation, it seems useful to entirely neglect this sensitivity of the shear stress at a surface to the shape of the velocity profile or, say, to the type of flow. Such a neglect entails that one might ascribe an additive nature to the shear stresses assigned to the two surfaces by formulae (1b) and (1c), i.e. in that the total shear stress at a surface may be found by summing the two component shear stresses shown in Fig. 2c: $\tau_a = \tau_o + \tau_1$ for the stationary surface and $\tau_b = \tau_o - \tau_1$ for the sliding one. Accordingly, formulae (1b) and (1c) can be rewritten as follows:

$$\frac{\tau_a}{\frac{1}{2}\rho u_m^2} = \frac{\tau_o + \tau_1}{\frac{1}{2}\rho u_m^2} = n\left(\frac{\rho u_m h}{\eta}\right)^m \qquad \text{for the } \underline{\text{stationary}} \text{ surface}$$

$$\frac{\tau_b}{\frac{1}{2}\rho(u_m - U)^2} = \frac{\tau_o - \tau_1}{\frac{1}{2}\rho(u_m - U)^2} = n\left\{\frac{\rho(u_m - U)h}{\eta}\right\}^m \qquad \text{for the } \underline{\text{sliding}} \text{ surface}$$

where τ_o = shear stress component due to the pressure flow component

τ_1 = shear stress component due to the drag flow component

U = sliding speed

u_m = mean flow velocity with respect to stationary surface

$u_m - U$ = mean flow velocity with respect to sliding surface.

On expressions for shear stress components τ_o and τ_1, a complete theory for turbulent lubricant films could then be built. However, it is not yet clear which values to select for n and m, even though it is known from the two limiting cases that their variations are fairly narrow, see formulae (2) and (3). Moreover, the above formulae are in a form that makes it obscure how to treat the most general cases where u_m and U are in intersecting direction, such as occurs due to side leakage in bearings having a finite width.

3. It is thus seen that the slight lack in consistency of different types of flow as regards their relationships between shear stress at a surface and average flow velocity relative to that surface, requires a more refined treatment than the one followed in establishing the two formulae sub Item No. 2. Such a refined treatment can be based on the notion that one might reduce the description of all combinations of both types of flow to a description in terms of only one type of flow, e.g. flow under the influence of a representative pressure gradient. This representative pressure gradient might then be put equal to the algebraic sum of the actual pressure gradient and of a fictitious one which accounts for the drag flow component.

In this refined treatment, it should be taken into account that, for one and the same average flow velocity, density, viscosity and film thickness, in either limiting case represented by formulae (2) or (3), wall-shear stress for one type of flow is not exactly equivalent with wall-shear stress for the other type of flow. In fact, the two shear stresses, although not differing to any appreciable extent, show a ratio different from unity. This ratio may be assessed by dividing formula (2) by formula (3) and assuming $u_{m_o} = u_{m_1}$ as well as identical values of ρ, η, h for the two cases, and replacing u_{m_o} and u_{m_1} by their common value u_m, viz.,

$$\frac{\tau_o}{\tau_1} = \frac{n_o}{n_1} \left(\frac{\rho u_m h}{\eta}\right)^{m_o - m_1} \qquad (4a)$$

where suffix 0 stands again for pressure flow and suffix 1 for drag flow. In the operational range so far explored, this ratio proves not to deviate appreciably from unity. It is readily seen that the ratio still depends on the Reynolds number, albeit raised to the very small power $m_o - m_1$ as follows:

$$\left(\frac{\rho u_m h}{\eta}\right)^{m_o - m_1}$$

In anticipation of experimental results still to be discussed, and which will show m_o and m_1 to be equal within the measuring error, it is assumed that the possible error of the approximation involved

in putting m_o and m_1 equal may be ignored.

Under this assumption it follows from formulae (2) and (3), when putting $u_{m_o} = u_{m_1}$ $m_o = m_1$ and introducing identical ρ, η, h for the two cases, that

$$\frac{\tau_o}{\tau_1} = \frac{n_o}{n_1} = a \qquad (4b)$$

in which a can be regarded to be a weighting factor.

Since in lubricant films the pressure build-up is of major importance, the description of combinations of the two types of flow will henceforth be simplified to the description of only one type of flow, namely the flow under the influence of a representative pressure gradient $(\frac{dp_r}{dx})$, in which the influence of the drag flow component on the shear stress is included. That is, in order to account for the occurrence of the drag flow component, a fictitious pressure gradient $(\frac{dp_1}{dx})$ will be introduced and it will be added to the actual pressure gradient $(\frac{dp}{dx})$ so as to obtain a representative gradient. Weighting factor $a = \frac{n_o}{n_1}$ in formula (4b) will be used when converting the shear stresses τ_1, which are due to the drag flow component, to the shear stresses $(a\tau_1)$ that are ascribed to a fictitious pressure flow component, characterized by an equally fictitious pressure gradient $(\frac{dp_1}{dx})$.

For the pressure flow in the steady state to which we will here confine ourselves, it follows from the equilibrium between the actual shear stress τ_o acting on elements dx on the two surfaces and the actual pressures p and p + dp acting on film thickness h that $2\tau_o dx = ph - (p+dp)h$. Thus,

$$\tau_o = -\frac{1}{2}\frac{dp}{dx} h \qquad (5a)$$

In analogy, for drag flow, the following relationship is introduced for defining the fictitious pressure gradient $(\frac{dp_1}{dx})$, which is henceforth taken representative of drag flow

$$a\tau_1 = -\frac{1}{2}\frac{dp_1}{dx} h, \text{ so that } \frac{dp_1}{dx} = -2a\frac{\tau_1}{h} \qquad (5b)$$

where a is the weighting factor defined in formula (4b).

Next we will consider the situation where both the pressure flow and the drag flow are present in the same film and where these components of flow are in parallel directions, see Fig. 2c. The actual shear stress at the stationary surface is $\tau_a = \tau_o + \tau_1$ (τ_o = shear stress under the influence of the pressure flow component; τ_1 = shear stress due to the drag flow component), whilst the actual shear stress at the sliding surface is $\tau_b = \tau_o - \tau_1$. For the reasons explained above, it seems justified to multiply the shear stress component (τ_1) due to drag flow by the weighting factor a of formula (4b), so that representative pressure gradients $\frac{dp_{ra}}{dx}$ and $\frac{dp_{rb}}{dx}$ for stationary and sliding surface may be attributed to $\tau_o + a\tau_1$ and $\tau_o - a\tau_1$, respectively.

At the stationary surface we then have:

$$\tau_o + a\tau_1 = -\frac{h}{2}\frac{d}{dx}(p+p_1);$$

which does contain the representative pressure gradient $\frac{d(p+p_1)}{dx} = \frac{dp_{ra}}{dx}$ generating flow with average flow velocity u_m relative to the stationary surface.

It follows from formulae (1) and (2) for the stationary surface that

$$\frac{-h\frac{d}{dx}(p+p_1)}{\rho u_m^2} = n_o\left(\frac{\rho u_m h}{\eta}\right)^{m_o} \qquad (6a)$$

At the sliding surface we may put:

$$\tau_o - a\tau_1 = -\frac{h}{2}\frac{d}{dx}(p-p_1).$$

This gives the representative pressure gradient $\frac{d(p-p_1)}{dx} = \frac{dp_{rb}}{dx}$ generating flow with average flow velocity $(u_m - U)$ relative to the sliding surface (in which U sliding speed).

It follows for the sliding surface from formulae (1) and (2)

$$\frac{-h\frac{d}{dx}(p-p_1)}{\rho(u_m-U)^2} = n_o\left\{\frac{\rho(u_m-U)h}{\eta}\right\}^{m_o} \qquad (6b)$$

The fictitious pressure gradient can be eliminated from these two formulae (6a) and (6b). Thus, the actual pressure gradient can be determined for any combination of pressure flow and drag flow, provided that average velocity u_m and sliding speed U have parallel directions, as has tacitly been assumed above:

$$\frac{dp}{dx} = -\frac{1}{2}n_o\left[\frac{\rho u_m^2}{h}\left(\frac{\rho u_m h}{\eta}\right)^{m_o} + \frac{\rho(u_m-U)^2}{h}\left\{\frac{\rho(u_m-U)h}{\eta}\right\}^{m_o}\right] \qquad (6c)$$

If the inertia effects other than those inherent in the turbulence character of the flow are negligible, it is now possible to forthwith determine the pressure build-up and load-carrying capacity of bearings having no side leakage (which would result in cross-flow) i.e. bearings having infinite width. It is remarkable that, by eliminating the fictitious pressure gradient, the magnitude of weighting factor a in formula (4b) or of factor n_1 in formula (3) does not affect in any way the magnitude of the actual pressure gradient in (6c).

One may also eliminate the actual pressure gradient from (6a) and (6b) and obtain the following expression for the fictitious pressure gradient

$$\frac{dp_1}{dx} = -\frac{1}{2}n_o\left[\frac{\rho u_m^2}{h}\left(\frac{\rho u_m h}{\eta}\right)^{m_o} - \frac{\rho(u_m-U)^2}{h}\left\{\frac{\rho(u_m-U)h}{\eta}\right\}^{m_o}\right], \qquad (6d)$$

In formula (5b)

$$\frac{dp_1}{dx} = -2a\frac{\tau_1}{h} = -2\frac{n_o}{n_1}\frac{\tau_1}{h}$$

the importance of weighting factor a does become evident.

Then, shear stress due to drag flow can be derived:

$$\tau_1 = \frac{1}{4}n_1\left[\rho u_m^2\left(\frac{\rho u_m h}{\eta}\right)^{m_o} - \rho(u_m-U)^2\left\{\frac{\rho(u_m-U)h}{\eta}\right\}^{m_o}\right] \qquad (6e)$$

Thus, empirical constant n_1 appears to be tied up with expressions for shear stress due to drag flow in the same way as previously shown

in the less general formula (3). For that matter, empirical constant n_o appears to be tied up with actual pressure gradients and shear stresses due to actual pressure gradients, see formula (6c) and the less general formula (2).

The above method of determining the pressure build-up in a turbulent lubricant film of infinite width can be generalized to lubricant films of finite width, i.e. with "cross-flow" where the pressure flow component and the drag flow component are not parallel to each other.

To this end it is assumed:

(1) that a fictitious pressure component may still be conceived in the lubricant film so as to account for the drag flow component;

(2) that for the stationary surface a relation can be given between, on the one hand, the gradient of the representative pressure being the algebraic sum of the actual pressure plus the additional fictitious pressure, and, on the other hand, the mean velocity of flow relative to the stationary surface, the density, the viscosity, and the film thickness, in accordance with equation (6a);

(3) that for the sliding surface a relation can be given between, on the one hand, the gradient of the representative total pressure being the algebraic sum of actual pressure minus the fictitious pressure and, on the other hand, the mean velocity of flow relative to the sliding surface, the density, the viscosity and the film thickness, in accordance with equation (6b);

(4) that the total or resultant representative gradient, $\frac{dp_r}{ds}$, and the resultant mean velocity of flow, u_s, for one and the same surface have the same direction;

(5) that such directions for stationary and sliding surface will not necessarily coincide.

These assumptions, and (4) and (5) in particular, lead to the following slightly generalized form of (6a) and (6b):

$$\frac{-h\frac{dp_r}{ds}}{\rho u_s^2} = n_o \left(\frac{\rho u_s h}{\eta}\right)^{m_o}$$

- where co-ordinate s and suffix s indicate the common direction of the resultant pressure gradient and the resultant mean flow velocity;
- where for the stationary surface, the pressure gradient $\frac{dp_{ra}}{ds}$ is the vectorial resultant of components $\frac{\partial(p_o+p_1)}{\partial x}$ and $\frac{\partial(p_o+p_1)}{\partial y}$, and where mean velocity u_s is the vectorial resultant of components u_x and u_y;
- where, for the sliding surface, the pressure gradient $\frac{dp_{rb}}{dr}$ is the vectorial resultant of components $\frac{\partial(p_o-p_1)}{\partial x}$ and $\frac{\partial(p_o-p_1)}{\partial y}$, and where mean velocity u_s is the vectorial resultant of flow components (u_x-U) and u_y.
- where the x-y co-ordinate system lies in the plane of, and is attached to, the stationary surface;
- where x is the sliding direction;
- where the y direction is at right angles to the sliding direction;
- and where u_x and u_y are the mean velocities of flow relative to the x- and y-directions, respectively.

Thus, equations for the stationary and the sliding surface can be derived:

(1) Stationary surface. By suitable resolving the resultant representative pressure gradient $\frac{dp_{ra}}{ds} = \frac{d(p_o+p_1)}{ds}$ and the resultant mean flow velocity $u_s=(u_x^2+u_y^2)^{\frac{1}{2}}$ in x and y-directions, it follows from formula (6f)

$$\frac{-h\frac{\partial}{\partial x}(p+p_1)}{\rho u_x(u_x^2+u_y^2)^{1/2}} = n_o\left\{\frac{\rho(u_x^2+u_y^2)^{1/2}h}{\eta}\right\}^{m_o} \qquad (7a)$$

$$\frac{-h\frac{\partial}{\partial y}(p+p_1)}{\rho u_y(u_x^2+u_y^2)^{1/2}} = n_o\left\{\frac{\rho(u_x^2+u_y^2)^{1/2}h}{\eta}\right\}^{m_o} \qquad (7b)$$

(2) Sliding surface. By suitable resolving the resultant gradient $\frac{dp_{rb}}{ds} = \frac{d(p_o - p_1)}{ds}$ and velocity $u_s = \{(u_x - U)^2 + u_y^2\}^{\frac{1}{2}}$ in x and y directions, it follows from formula (6f)

$$\frac{-h \frac{\partial}{\partial x}(p-p_1)}{\rho(u_x-U)\{(u_x-U)^2+u_y^2\}^{1/2}} = n_o\left[\frac{\rho\{(u_x-U)^2+u_y^2\}^{1/2}\, h}{\eta}\right]^{m_o} \qquad (7c)$$

$$\frac{-h \frac{\partial}{\partial y}(p-p_1)}{\rho u_y\{(u_x-U)^2+u_y^2\}^{1/2}} = n_o\left[\frac{\rho\{(u_x-U)^2+u_y^2\}^{1/2}\, h}{\eta}\right]^{m_o} \qquad (7d)$$

In the original limiting case of parallel flow directions (where the flow component u_y, at right angles to the sliding direction of the surface, reduces to zero), equation (7a) indeed reduces to (6a) and equation (7c) to (6b).

Equations (7a-d) have been written in such a way that the fictitious pressure gradients can be easily eliminated. Therefrom, equations can be derived that yield gradients of the actual pressure in the lubricant film, as follows:

$$-\frac{h^2}{\eta U}\frac{\partial p}{\partial x}\left(\frac{\eta}{\rho U h}\right)^{1+m_o} =$$

$$= \frac{1}{2} n_o\left[U_x(U_x^2+U_y^2)^{\frac{1+m_o}{2}} + (U_x-1)\{(U_x-1)^2+U_y^2\}^{\frac{1+m_o}{2}}\right] \qquad (8a)$$

$$-\frac{h^2}{\eta U}\frac{\partial p}{\partial y}\left(\frac{\eta}{\rho U h}\right)^{1+m_o} =$$

$$= \frac{1}{2} n_o\left[U_y(U_x^2+U_y^2)^{\frac{1+m_o}{2}} + U_y\{(U_x-1)^2+U_y^2\}^{\frac{1+m_o}{2}}\right] \qquad (8b)$$

where

$U_x = \frac{u_x}{U}$ and $U_y = \frac{u_y}{U}$ are normalized velocities of flow. (8b)

This way of formulating the basic equations for the turbulent lubricant film has advantages in comparing theoretical and experimental results. It can be shown from the above derivation that only a minimum of experimental information is required for proving the theory to be valid and determining the empirical constants.

(a) We should be able to derive the magnitudes of n_o and m_o from simple experiments with unidirectional types of turbulent flows (see formula (2)). One may confine oneself even to a flow experiment in which pressure flow, i.e. under the influence of a pressure gradient, is the only type of flow to occur. It is particularly the magnitude of n_o that matters. The magnitude of m_o need not be known accurately, provided its absolute value is much smaller than unity, since in the formulae (8a) and (8b) it appears only to the $\frac{1}{2}(1+m_o)$th power.

(b) We should be able to derive the quantities n_1 and m_1 (see formula (3)) from experiments with drag flow, i.e. due to the sliding of one of the two surfaces. If however, only the pressure build-up in a bearing is required, it would suffice to determine whether n_1 and m_1 do not deviate too much from n_o and m_o, respectively. In fact, it proved possible, thanks to the introduction of a fictitious pressure, to derive the equations (8a) and (8b) for the pressure build-up in which the quantities n_1 and m_1 no longer appear.

A disadvantage of the above way of formulating equations for flow in the turbulent lubricant film might be the fact that average flow velocities are not known a priori. Accordingly, these equations cannot be inserted in the equations expressing the continuity condition to yield differential equations for the pressure build-up. A feasible way of formulating such differential equations is given in appendix 1.

Another disadvantage of the above two equations might be the fact that one of the two bearing surfaces has been assumed to be stationary. In many bearings either surface might move with respect to the lubricant film as a body, and for physical visualization it is convenient to attach a new frame of reference $\underline{x}$, $\underline{y}$ to the body of the film. Now, let the velocity of the new co-ordinate system ($\underline{x}$, $\underline{y}$) be in the x-direction. Further, let the meaning of symbol U no longer be restricted to sliding speed as in the previous frame of reference but let the meaning of it be extended to the sum of the

speeds of the two surfaces (u_1 and u_2) with respect to the new co-ordinate system $\underline{x}$, $\underline{y}$:
$U = u_1 + u_2$ or, in normalized form, $U_1 + U_2 = 1$ and $U_{\underline{y}} = U_y$, $U_{\underline{x}} = U_x + U_1$.

This generalizing transformation yields:

$$-\frac{h^2}{\eta U}\frac{\partial p}{\partial \underline{x}}\left(\frac{\eta}{\rho U h}\right)^{1+m_o}$$

$$= \frac{1}{2}\, n_o \left[(U_{\underline{x}} - U_1)\left\{(U_{\underline{x}} - U_1)^2 + U_{\underline{y}}^2\right\}^{\frac{1+m_o}{2}} + (U_{\underline{x}} - U_2)\left\{(U_{\underline{x}} - U_2)^2 + U_{\underline{y}}^2\right\}^{\frac{1+m_o}{2}} \right] \qquad (9a)$$

$$-\frac{h^2}{\eta U}\frac{\partial p}{\partial \underline{y}}\left(\frac{\eta}{\rho U h}\right)^{1+m_o}$$

$$= \frac{1}{2}\, n_o \left[U_{\underline{y}}\left\{(U_{\underline{x}} - U_1)^2 + U_{\underline{y}}^2\right\}^{\frac{1+m_o}{2}} + U_{\underline{y}}\left\{(U_{\underline{x}} - U_2)^2 + U_{\underline{y}}^2\right\}^{\frac{1+m_o}{2}} \right] \qquad (9b)$$

and $U_1 + U_2 = 1 \qquad (9c)$

The presence of inertia effects other than those inherent in turbulence may be incorporated most concisely in equations (9a) and (9b) thanks to the facts that the pressure is explicit and that the co-ordinate system is stationary with respect to the shape of the wedge. To account for these inertia effects the following terms must be added to the righthand side of equations (9a) and (9b)

$$+\left(\frac{\eta}{\rho U h_o}\right)^{m_o}\left\{\frac{h}{U}\frac{\partial U_{\underline{x}}}{\partial t} + hU_{\underline{x}}\frac{\partial U_{\underline{x}}}{\partial \underline{x}} + hU_{\underline{y}}\frac{\partial U_{\underline{x}}}{\partial \underline{y}}\right\} \qquad (10a)$$

and

$$+\left(\frac{\eta}{\rho U h_o}\right)^{m_o}\left\{\frac{h}{U}\frac{\partial U_{\underline{y}}}{\partial t} + hU_{\underline{x}}\frac{\partial U_{\underline{y}}}{\partial \underline{x}} + hU_{\underline{y}}\frac{\partial U_{\underline{y}}}{\partial \underline{y}}\right\} \qquad (10b)$$

respectively.[1] In terms (10a) and (10b) the acceleration terms ($\frac{\partial U_{\underline{x}}}{\partial t}$, etc.) are correct from a physical viewpoint. However, the kinetic energy terms ($U_{\underline{x}}\frac{\partial U_{\underline{x}}}{\partial \underline{x}}$, etc.) are not entirely correct and may be underestimated. This is due to the fact that the products of average flow velocities $U_{\underline{x}}$ and $U_{\underline{y}}$ are inserted in (10a) and (10b). It would have been more correct to insert products of local flow velocities and to take averages of these products. But profiles of the local flow velocities are known to be rather blunt. Thus, the difference between the product of two average velocities and the average of the product of two local velocities may be expected to be small. Indeed, kinetic energy terms are underestimated by probably less than 20 per cent[2]. Such an error is permissible if the kinetic energy terms are a first or higher order effect as far as pressure build-up is concerned.

In view of the fact that solving the generalized equations (9a+10a) and (9b+10b) for the pressure distribution might well prove difficult, it seems sensible to take a look in the first place at bearing designs which make such a solution unnecessary. Let us thereafter confine ourselves to bearing designs in which these inertia effects constitute merely a first order effect. It makes sense to do this since:

(a) In probably a large number of cases inertia effects other than turbulence, e.g. kinetic energy terms, may well prove negligible. Indeed, it can be imagined that the following conditions exist simultaneously in lubricant films

large $n_o\left(\frac{\rho U h}{\eta}\right)^{m_o}$, which is characteristic of rough surfaces

small $\frac{(U_{\underline{x}})_{max}}{(U_{\underline{x}})_{min}}$ and $\frac{(U_{\underline{y}})_{max}}{(U_{\underline{y}})_{min}}$, which is characteristic of bearings without grooves, or only with shallow grooves, and with parallel, or only slightly non-parallel, surfaces.

[1]) Where all inertia effects induced by curvature of the film, e.g. around a journal, have been ignored.

[2]) For pressure flow, i.e. under the sole influence of a pressure gradient, the underestimate amounts to 10 per cent.

and small $\frac{h}{x}$ and $\frac{h}{y}$, which is characteristic of bearings with small ratios of film thickness and overall dimensions. It will be obvious that in such cases inertia effects may be neglected.

(b) It is perhaps possible to adapt the semi-empirical formulae (9a) and (9b) to the presence of inertia effects other than turbulence by suitable adaptation of the constants n_o and m_o.

Through introducing a new dimensionless parameter

$$\alpha = \frac{h}{d}\frac{1}{n_o}\left(\frac{\eta}{\rho U h}\right)^{m_o} \qquad (10c)$$

a more straightforward way of treating inertia effects is possible; i.e. by observing that

1. inertia effects are small if the dimensionless parameter (α) is much smaller than unity
2. in that case inertia effects can be regarded to be a first order effect:

   $p = p_{turb.} + \alpha p_{inertia}$.

All this leads to a simplification of analytical work:

a. when $\alpha \sim 0.01$, inertia effects other than turbulence can be neglected

b. when $\alpha \sim 0.1$, inertia effects are a first order effect, and a corresponding correction will probably prove to be far from appreciable.

No simplification seems possible if the order of magnitude of α is unity. At values of α greater than unity, the validity of the formulae derived in this chapter becomes doubtful.

6. EXPERIMENTAL VERIFICATION OF THE BULK-FLOW THEORY

The present semi-empirical theory of the turbulent lubricant film can only be verified on the basis of a large number of experimental results. Especially when direct adaptation of formulae (8a) and of (8b) to the presence of inertia effects is required, a great amount of experimental work must still be done. It can be stated right now that but a rather small amount of this work can be found in literature. Since it will be useful to handle experimental results more or less systematically and to get some idea of the amount of experimental work yet to be done, the following classification system has been set up for the turbulent film:

I Types of film flow

1 "Pressure flow" under the influence of a pressure gradient
2 "Drag flow" due to the sliding of a surface
3 A combination of the two main types of flow in parallel directions
4 A combination of the two main types of flow in directions including an angle.

II Lubricant film profile without roughness and/or patterns of shallow grooves in the surfaces

10 Plane lubricant film
20 Curved lubricant film, uniform film thickness
30 Plane lubricant film, non-uniform film thickness
40 Curved lubricant film, non-uniform film thickness.

III Surface finish

100 Both surfaces smooth
200 One surface smooth, the other being rough
300 Both surfaces rough.

IV Smallscale design characteristics of the surfaces

1000 Both surfaces ungrooved
2000 One surface ungrooved, the other having a large number of shallow grooves
3000 Both surfaces have a large number of shallow grooves.

On the basis of this classification system it is possible to give a systematical survey of experimental data found in literature. Almost all data will be seen to be characteristic of smooth ungrooved surfaces (1100). Within this category, sixteen combinations of types of flow and film profile can be formed on the basis of the above classification system. Nine combinations could be found in literature (see Table 1 on page 43). It will be seen that they are the more significant combinations out of the sixteen possible combinations. However, enough experimental data for strongly non-parallel surfaces are lacking. One of the combinations, i.e. 1134, is particularly important because practical bearings fall in this category.

The experimental data, classified along the lines indicated above, should provide us with the proofs that the step-by-step generalizations of formula (1a)

$$\frac{\tau}{\frac{1}{2}\rho u_m^2} = n\left(\frac{\rho u_m h}{\eta}\right)^m ,$$

which has elaborately been outlined in the previous chapter, is justified. The generalization is in 4 steps, and follows the classification of types of film flow (see also Table 1):

1. Pressure flow. Experiments on this flow type should provide us with fitted values for constants n_o and m_o in formula (2).
2. Drag flow. Experiments should provide us with fitted values for constants n_1 and m_1 in formula (3). The generalization of the above formula (1a) would appear justified if $m_o \approx m_1$, and $n_o/n_1 = a \approx 1$, see formula (4a-b).
3. Combination of the two main types of flow in parallel directions. Using the constants n_o, m_o, n_1 and m_1, pressure gradient and wall shear stress must be correctly predicted by formula (6a-e).
4. Combinations of the two main types of flow in directions including an angle. This description includes the flow pattern occurring in practical bearings. Using the constants n_o, m_o, n_1, and m_1, pressure gradient and wall shear stress must be correctly predicted by formulae (7a-d) and (8a-b).

Classification	ıin	Re_{max}	agreement theory experiment
1111	Pr fi gr 10^3	10^5	good
1112	Dr th 10^3	$3\cdot10^4$	good
1113	Co pa fo gr 10^3	$3\cdot10^4$	good
1121	Pr fi gr 10^3	10^5	fair
1122	Dr 10^3 fi 10^3 gr 10^3	$6\cdot10^3$ $2\cdot10^4$	fair
1123	Cc pa fc ur 10^3	$2.4\cdot10^3$	good
1124	Cc di fi fe 10^3	$2\cdot10^4$	fair
1134 bearing test	Cc di fi fe 10^3	$1.2\cdot10^4$	good
1143	Cc pa nc ar 10^3	$3.2\cdot10^3$	good
1311	Pı fi		
2124	Cc di fi sn 10^3	$6\cdot10^3$	good

) This critical Reynolds number is a function of n_o, see sub 1134.

Classification		test of formula	experimental results	ratio	Re_{min}	Re_{max}	agreement theory experiment
1111	Pressure flow, plane lubricant film and uniform film thickness, both surfaces smooth and ungrooved	2	n_o=0.066 m_o= -0.25	$\frac{h}{r}$=0	10^3	10^5	good
1112	Drag flow, plane lubricant film and uniform film thickness, both surfaces smooth and ungrooved	3,4a-b	n_1=0.055 m_1=-0.25	$\frac{h}{r}$=0	10^3	$3\cdot10^4$	good
1113	Combination of the two main types of flow in parallel directions, plane lubricant film and uniform film thickness, both surfaces smooth and ungrooved	6a - b for u_m= 0	n_o=0.066 m_o=-0.25 n_1=0.055 m_1=-0.25	?	$3\cdot10^3$	$3\cdot10^4$	good
1121	Pressure flow, curved lubricant film and uniform film thickness, both surfaces smooth and ungrooved	?	$0.066 < n_o < 0.088$ m_o=-0.25	$\frac{h}{r} < 0.03$	10^3	10^5	fair
1122	Drag flow, curved lubricant film and uniform film thickness, both surfaces smooth and ungrooved	3,4a-b	n_1=0.065 m_1=-0.25 n_1=0.065 " n_1=0.085 "	$\frac{h}{r}$=0.016 $\frac{h}{r}$=0.028 $\frac{h}{r}$=0.099	10^3 $5\cdot10^3$ $5\cdot10^3$	$6\cdot10^3$ $2\cdot10^4$	fair
1123	Combination of the two main types of flow in parallel directions, curved lubricant film, uniform film thickness, both surfaces smooth and ungrooved	6c for $u_m=\frac{1}{4}U$	n_o=0.066 m_1=-0.25	$\frac{h}{r}$=0.016	$2.4\cdot10^3$	$2.4\cdot10^3$	good
1124	Combination of the two main types of flow in directions including an angle, curved lubricant film and uniform film thickness, both surfaces smooth and ungrooved	8b for $U_x=\frac{1}{2}$	n_o=0.052 m_o=-0.24	$\frac{h}{r}$=0.014-0.115	10^3	$2\cdot10^4$	fair
1134 bearing test	Combination of the two main types of flow in directions including an angle, plane lubricant film and non-uniform film thickness, both surfaces smooth and ungrooved	8a-b	$(\frac{\rho Uh}{\eta})_c$=[1]) 1,000 m_o=-0.25	$\frac{h}{r}$= 0.003	$2\cdot10^3$	$1.2\cdot10^4$	good
1143	Combination of the two main types of flow in parallel directions, curved lubricant film and non-uniform film thickness, both surfaces smooth and ungrooved	6c	n_o=0.066 m_o=-0.25	$\frac{h}{r}$=0.01	$2.4\cdot10^3$	$3.2\cdot10^3$	good
1311	Pressure flow, plane lubricant film and uniform film thickness both surfaces rough and ungrooved	1	$-0.25 < m_o < 0$				
2124	Combination of the two main types of flow in directions including an angle, curved lubricant film, uniform film thickness, both surfaces smooth and grooved	8a-b	$(\frac{\rho Uh}{\eta})_c \approx 500$[1]) m_o=-0.25	$\frac{h}{r}$= 0.004	10^3	$6\cdot10^3$	good

[1]) This critical Reynolds number is a function of n_o, see sub 1134.

Table 1

Moreover, the load-carrying capacity of a bearing must be correctly predicted by the solution found for the pressure by integrating formulae (8a-b) in conjunction with the continuity condition.

In the accompanying Table 1 experimental results pertinent to the generalization of formula (1a) are collected. It can be seen that sufficient experimental proofs for the bulk-flow theory could be collected for smooth ungrooved surfaces with both plane and curved lubricant films.

The remaining two experiments, one with rough and the other with grooved surfaces, do not suffice for generally proving the theory. However, with grooved surfaces, there exists agreement between theory and experiment for a complicated combination of the two main flow types. Then one may be confident that the theory will at least be also valid for grooved surfaces.

Details of the experiments of Table 1 are dealt with in the rest of the present chapter.

1111 Pressure flow, plane lubricant film and uniform film thickness, both surfaces smooth and ungrooved.

Of the many experimental results obtained with turbulent flow between two surfaces those of Davies and White (1929) have been selected. From these tests the values of the constants in formula (2) relating friction-factor and Reynolds number can be derived. For Reynolds numbers

$$\frac{\rho u_m h}{\eta} \text{ smaller than } 10^5 \text{ we find:}$$

$$n_o = 0.066 \text{ and } m_o = -0.25.$$

In a book by Schlichting (1965) and a survey article by Hartnett, Koh and Mc Comas (1962), it was shown that the hydraulic diameter concept is valid when comparing experimental results with pipes and between two surfaces. This concept enabled the author to derive the same two above values for the experimental constants n_o and m_o from experiments on turbulent flow in the annular space formed by two concentric round pipes (Koch and Feind, 1958) and from the basic experiments on flow in round pipes by Blasius (1913). All the experiments cited here indicate that the above two values for n_o and m_o are valid up to

Reynolds numbers of 10^5. At higher Reynolds numbers slightly different values will be found.

1112 Drag flow, plane lubricant film, and uniform film thickness, both surfaces smooth and ungrooved.

Only two tests, one by Couette (1890) and the other, by Robertson (1959), come in this category. The results of these two test series agree surprisingly well with each other. The values of the constants in formula (3) can be derived from these tests. Up to the highest Reynolds number at which these measurements were made, i.e. $\frac{\rho u_m h}{\eta} \approx 30{,}000$, we find: $n_1 = 0.055$ and $m_1 = -0.25$.

True, on the sole basis of the experiments by Robertson it might be derived that the value for m_1 might be smaller: $m_1 = -0.2$. However, the author felt that the range of Reynolds numbers covered by Robertson 10^4-3 10^4 was not sufficiently wide and that values for n_1 and m_1 should rather be so taken as to yield the best correlation for the entire range covered together by Robertson (1959) and Couette (1890).

It is to be observed that only Robertson used a plane film. Couette used a stationary shaft and a rotating bearing with a small radial clearance to radius ratio. But in such cases turbulent Couette flow is physically almost identical to turbulent plane flow.

Robertson's measurements of the friction factor are indirect, being derived from measured flow velocity profiles. Couette's measurements are direct in that he measured the torque exerted on the shaft.

1113 Combination of the two main types of flow in parallel directions, plane lubricant film and uniform film thickness, both surfaces smooth and ungrooved.

Only the results derived from Shinkle and Hornung's test series (1965) are given here. In their test series the flow relative to the stationary surface was blocked by a barrage attached to the stationary surface, hence $u_m = 0$. The shear stress $\tau_b = \tau_o - \tau_1$ at the sliding surface (τ_o due to the pressure flow component and τ_1 due to the drag flow component) was measured, see Fig. 2. Their results are given in a graph and they can very well be represented by the following formula:

$$\frac{\tau_b}{\frac{1}{2}\rho U^2} = -0.062 \left(\frac{\rho U h}{\eta}\right)^{-0.25}$$

for $3{,}000 < \frac{\rho U h}{\eta} < 30{,}000$ and in which $\tau_b = \tau_o - \tau_1$.

For comparison a formula of the same form will now be derived from 6a and b. From the tests described sub 1111 and 1112, it was found that:

$m_o = m_1 = -0.25$

$n_o = 0.066$, $\quad n_1 = 0.055$, so that $a = \frac{n_o}{n_1} = 1.2$.

Substituting these values in formulae (6a and b) and taking account of the fact that the mean velocity of flow u_m relative to the stationary surface is blocked, ($u_m = 0$) gives:

$$\frac{d(p+p_1)}{dx} = 0$$

$$\frac{-h \frac{d}{dx}(p-p_1)}{\rho U^2} = -0.066 \left(\frac{\rho U h}{\eta}\right)^{-0.25}$$

$$\tau_o = -\frac{1}{2}\frac{dp}{dx} h \qquad \text{and} \qquad 1.2\tau_1 = -\frac{1}{2}\frac{dp_1}{dx} h$$

thus $$\frac{\tau_o}{\frac{1}{2}\rho U^2} = -0.033 \left(\frac{\rho U h}{\eta}\right)^{-0.25}$$

and $$\frac{\tau_1}{\frac{1}{2}\rho U^2} = 0.0275 \left(\frac{\rho U h}{\eta}\right)^{-0.25}$$

Hence,

$$\frac{\tau_b}{\frac{1}{2}\rho U^2} = -0.060 \left(\frac{\rho U h}{\eta}\right)^{-0.25}$$

in which $\tau_b = \tau_o - \tau_1$ agrees surprisingly well with the above formula derived from Shinkle and Hornung's tests.

It should be noted that for $\frac{\rho U h}{\eta} > 30{,}000$, in Shinkle and Hornung's test series showed, the influence of measuring errors, of roughness of the surface, or of inertia effects in the flow other

than those inherent in turbulence, become apparent. Consequently, at $\frac{\rho U h}{\eta}$ = 100,000 the theoretical value is 15 % lower than the experimental value. However, in the aforementioned regime of Reynolds numbers greater than 3,000 and smaller than 30,000 excellent agreement has been found.

Strictly speaking, the experiments here surveyed do not come into category 1113 because the lubricant film had a curved profile. However, in Shinkle and Hornung's test series the effect of the curvature was negligible because the mean velocity of flow in circumferential direction was zero: $u_m = 0$.

1121 Pressure flow, curved lubricant film and uniform film thickness, both surfaces smooth and ungrooved.

No experiments are known that are directly related with the present case. However, the many measurements published for curved pipes enable us to gain an insight into the effect of curvature of the surfaces on the flow, particularly into the inertia effects associated with the curvature. It will be evident that we need only consider those cases in which the radius r_1 of the pipe is small with respect to the radius r of the curvature. In fact, in bearings, the ratio between the lubricant film thickness and the radius of curvature will invariably be exceedingly small ($\sim 0.003 < \frac{h}{r} < \sim 0.03$). It may be expected that the effect of the curvature in such cases will be evident from a moderate increase in flow resistance or, say, in the pressure differential required for maintaining a given flow.

According to tests by White (1932) and Ito (1959), the ratio between pressure drop with flow in a curved pipe and in a straight one can, for the range covered by them, be expressed by:

$$a_o + a_1 \left(\frac{\rho u_m r_1}{\eta}\right)^{1/4} \left(\frac{r_1}{r}\right)^{1/2}$$

The values found for a_o and a_1 do not completely agree in these two test series. For our purpose it is sufficient to know that $a_o \sim 1$ and $a_1 \sim 0.1$. It can then be derived immediately that for

$$\frac{\rho u_m r_1}{\eta} < 10^5 \text{ and } \frac{r_1}{r} < 0.03$$

the curvature of the pipe causes an increase of pressure drop not exceeding 30 %. Keeping in mind that the Reynolds numbers and the film thickness to radius ratio in bearings certainly not reach the above values, we will in all the cases still to be described, in which the curvature of surfaces also plays a role, try to demonstrate that the effect of the curvature is small.

1122 Drag flow, curved lubricant film and uniform film thickness, both surfaces smooth and ungrooved.

Three test series come into this category. The authors are Burton (1967), Taylor (1923) and Pan and Vohr (1967). Tests by Burton (1967) with a bearing model with the rather large ratio of 0.016 between lubricant film thickness and radius include, among other things, indirect measurements of the shear stress at a surface due to drag flow. From his tests it can be concluded that for

$$1{,}000 < \frac{\rho u_m h}{\eta} < 6{,}000$$

the constants of formula (3) had the following values:

$$n_1 = 0.065 \text{ and } m_1 = -0.25.$$

As regards Burton's tests with the lower values of these Reynolds numbers, the constants, substituted in formula (3) gave somewhat too low values for the shear stress at the surface, i.e. down to -10 %. Probably these low values are due to an influence of Taylor vortices. Conditions for Taylor vortices to occur in a transition region between laminar and turbulent flow were favourable because Burton, as well as the other authors, used a rotating journal and a stationary bearing.

Taylor (1923) used a still greater lubricant film thickness to radius ratio in his tests, viz., $\frac{h}{r} = 0.028$. From his results the same values can be derived, viz., $n_1 = 0.065$ and $m_1 = -0.25$ for

$$\frac{\rho u_m h}{\eta} > 5000.$$

Finally, tests by Pan and Vohr (1967) should be mentioned, these showing the highest film thickness to radius ratio (much higher than the value which is desirable for bearings), viz., $\frac{h}{r} = 0.099$. From

their tests we can derive: $n_1 = 0.085$ and $m_1 = -0.25$ for

$$\frac{\rho u_m h}{\eta} > 5000.$$

It should also be noted that both from Taylor's and from Pan and Vohr's tests it follows that up to approximately

$$\frac{\rho u_m h}{\eta} = 5{,}000,$$

Taylor vortices may have had a considerable influence and that the shear stresses which can be predicted on the basis of the above mentioned constants, i.e. for

$$\frac{\rho u_m h}{\eta} < 5{,}000,$$ will be lower than the measured values. On the other hand, in Burton's tests the influence of vorticity was much less pronounced in this same range. Consequently, there might well have been some mechanism that suppressed vorticity in Burton's tests and due to which the transition to turbulent flow took place already at lower Reynolds numbers, somewhere in the neighbourhood of $\frac{\rho u_m h}{\eta} \sim 1{,}000$. A different explanation might lie in the fact that Burton derived shear stresses indirectly, namely from measured flow velocity profiles and that the influence of vorticity on shear stress becomes rather elusive by doing so.

The general conclusion is that the effect of the curvature is small and manifests itself in an increase of the constant n_1 by less than 20 per cent if $\frac{h}{r} < 0.03$ and that the increase may even be neglected altogether whenever $\frac{h}{r} \leq 0.003$. The values for constant m_1 remain unchanged. If Taylor vortices are present in the films, an estimate of the shear stress on the basis of the above values for constants n_1 and m_1 tends to be conservative. However, the influence of these vortices on shear stress will be confined to Reynolds numbers smaller than 5,000.

1123 Combination of the two main types of flow in parallel directions, curved lubricant film, uniform film thickness, both surfaces smooth and ungrooved.

In the literature the author could find only one test (Burton, 1967) in the present category. Burton has measured pressures in a

flow relative to the stationary surface; the flow was not entirely blocked, and u_m amounted to about 1/4 U. His test was made under conditions in which inertia effects at the inlet and outlet of the film played a considerable role.

Notwithstanding these inertia effects, it can be derived from a measurement at one Reynolds number that:

$$\frac{h^2}{\eta U}\frac{dp}{dx}\left(\frac{\eta}{\rho U h}\right)^{3/4} = 0.021 \pm 10\ \%.$$

By substituting $u_m = \frac{1}{4} U$ and $n_o = 0.066$, $m_o = -0.25$ [1]) in formula (6c) and by rearranging it follows that

$$\frac{h^2}{\eta U}\frac{dp}{dx}\left(\frac{\eta}{\rho U h}\right)^{3/4} = 0.017.$$

Hence the theoretical result when using values for n_o and m_o valid for plane films is somewhat lower than the experimental one. This might well be due to the fact that in Burton's experiment (1967) a shaft was rotating in a bearing with the rather great radial clearance to radius ratio of 0.016. Hence, the influence of the inertia effects induced by the curvature of the lubricant film again manifests itself in a moderate increase in pressure build-up, i.e. by about 20 percent.

1124 Combination of the two main types of flow in directions including an angle, curved lubricant film and uniform film thickness, both surfaces smooth and ungrooved.

Attention is given here in particular to the combination of pressure flow and drag flow in which both flow-components are at right angles to each other. This flow pattern obtains, for instance, when a shaft is made to rotate concentrically in a cylindrical bearing and when also a flow in axial direction between the surfaces is set up by an equally axial pressure gradient. This flow pattern was realized in tests by Tao and Donovan (1955) and by Yamada (1962). Only Yamada's tests are treated here because they seem to be more reliable and are interpreted more easily. Yamada represents the results of his measurements as follows:

$$\frac{\frac{dp}{dy}h}{\rho u_y^2} = f\left(\frac{\rho U h}{\eta}, \frac{\rho u_y h}{\eta}\right)$$

[1]) see sub 1111.

with u_y in the axial direction y, and U in the circumferential direction x. At neither surface did Yamada measure shear stresses in the circumferential direction. His tests were focused on measuring axial flow rate and axial pressure gradient at various rotational speeds.

From formula (8b) it is possible to derive an expression which lends itself to comparison with Yamada's experimental results.

To this end formula (8b) should first be adapted to the present condition where the average flow component in circumferential direction must have been equal to half the sliding velocity: $U_x = \frac{u_x}{U} = 0.5$. This accounts for the fact that there is no pressure flow component in the circumferential direction. After some calculation it then follows that:

$$\frac{\frac{dp}{dy}h}{\rho u_y^2} = -n_o\left(\frac{\rho u_y h}{\eta}\right)^{m_o}\left\{\frac{1}{4}\left(\frac{U}{u_y}\right)^2 + 1\right\}^{\frac{1+m_o}{2}}$$

or, by substituting $\lambda = \frac{4\frac{dp}{dy}h}{\rho u_y^2}$, $Re = \frac{\rho u_y h}{\eta}$

and $R_\omega = \frac{\rho U h}{\eta}$,

$$\lambda = 4\, n_o\, Re^{m_o}\left\{\frac{1}{4}\left(\frac{R_\omega}{Re}\right)^2 + 1\right\}^{\frac{1+m_o}{2}}$$

Sub category 1111, the following values for n_o and m_o with pressure flow have been found, $n_o = 0.066$ and $m_o = -0.25$. However, Yamada (1962) himself has found slightly different values: $n_o = 0.065$ and $m_o = -0.24$ for his particular experimental apparatus with pressure flow ($R_\omega = 0$). This discrepancy is probably due to a slight influence of inertia effects other than those inherent in turbulence. In Fig. 3, some of Yamada's experimental results have been depicted. It can clearly be seen that these results agree roughly with the above equation. For a few cases depicted in Fig. 3a and 3b a closer inspection of the agreement between theory (dotted lines) and experiment (drawn lines) is possible. The dotted, theoretical lines apply to the cases characterized by $R_\omega = 3{,}000$ and $5{,}000$ in Fig. 3a and $R_\omega = 10{,}000$ and $20{,}000$ in Fig. 3b and are based on the above equation when substi-

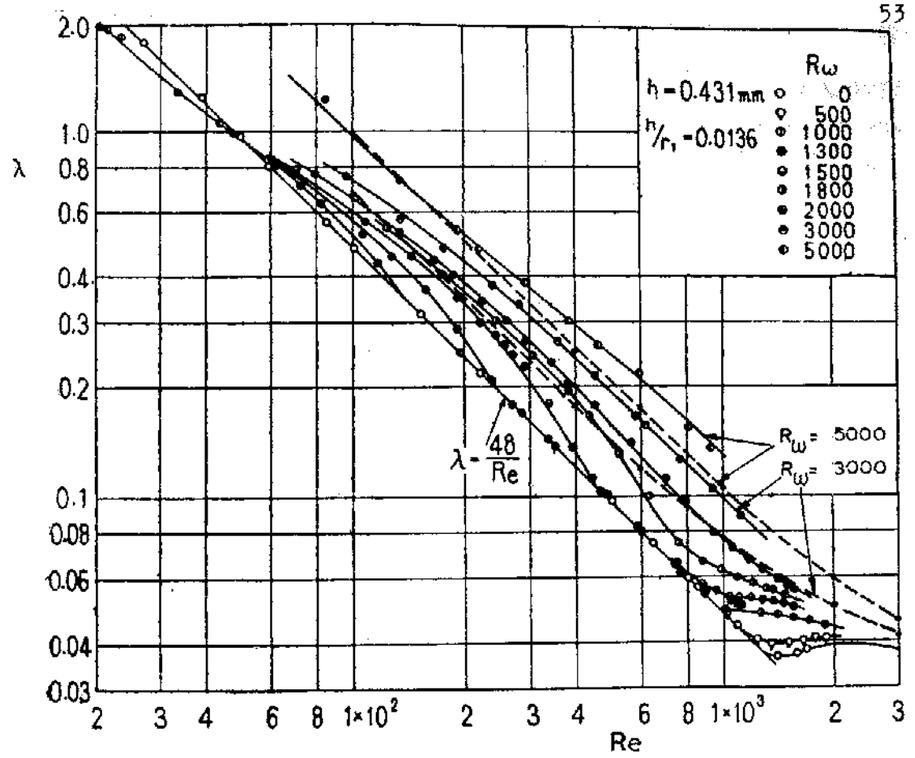

Fig.3 Relationship between $\lambda = \frac{4\frac{dp}{dy}h}{\rho u_y^2}$ and $Re = \frac{\rho u_y h}{\eta}$ with $R_\omega = \frac{\rho U h}{\eta}$ as parameter

tuting therein Yamada's own values for n_o and m_o. It can be seen that the agreement between theory and experiment is excellent for $R_\omega \gg Re$ and $Re \gg R_\omega$, or $U \gg u_y$ and $u_y \gg U$. But in a regime characterized by $Re \approx \frac{1}{2} R_\omega$, or $u_y \approx \frac{1}{2} U$, his experimental results are generally higher (about 20 per cent) than theoretical results. This effect can probably be attributed to Taylor vortices, but is so small that there is no immediate need to account for the occurrence of these vortices.

The above formulae which have been derived for the present, special category is identical to Tao and Donovan's and Yamada's formulae except for deviating values of some numerical constants. Their theoretical work relating to this special case can therefore be considered as a first attempt at developing a theory on the turbulent lubricant film and the more general equations that have already been outlined elaborately in the previous chapter.

1134 Combination of the two main types of flow in directions including an angle, plane lubricant film and non-uniform film thickness, both surfaces smooth and ungrooved.

A number of experiments are known with plain cylindrical fluid film bearings, Fig. 1a (Smith, Fuller (1965) and Ketola, Mc Hugh (1967)), and with tilting-pad bearings, Fig. 1c (Orcutt, (1967)). All these experiments may also be used here to verify the theory.

In these tests the film thickness to radius ratio was so small that the curvature of the lubricant film and inertia effects due to the wedge shape of the film may be neglected: $\frac{h}{r} \approx 10^{-3}$. Accurate comparison of theory and experiment is not yet possible since the equations (8a) and (8b) have not yet been solved. Indeed, in the first place it must still be shown that such solutions are useful and valid. It is possible, however, to make a rough comparison. Indeed, it can be derived from (8a) and (8b) that a solution of these equations should give a result of the following nature:

$$\frac{p_m h_o^2}{\eta U r} = \left(\frac{\rho U h_o}{\eta}\right)^{1+m_o} f_1(\varepsilon, \frac{b}{d})$$

where p_m = mean pressure over the projected surface b d

h_o = radial clearance

ε = dimensionless eccentricity $\frac{e}{h_o}$

$\frac{b}{d}$ = width/diameter ratio.

In the above-discussed category 1111, the numerical value of m_o was found: $m_o = -0.25$. For laminar flow in the lubricant film it is well known that:

$$\frac{p_m h_o^2}{\eta U r} = f_2(\varepsilon, \frac{b}{d}).$$

In appendix 2, the author has determined function $f_1(\varepsilon, b/d)$ in the former equation for one simple case, namely for an infinitely wide, plain journal bearing ($\frac{b}{d} \to \infty$). By way of an example, the case has been numerically worked out for one small value for the eccentricity ($\varepsilon = 0.2$) and the result has been compared with the numerical result following for the same case, but with laminar flow, from the latter equation.

As expected, there appears to exist a critical Reynolds number:

$$\left(\frac{\rho U h_o}{\eta}\right)_c$$

at which the two equations yield identical numerical results. This critical number represents the transition from laminar to turbulent flow as far as the calculation of load-carrying capacity is concerned. The value for this critical Reynolds number turns out to be:

$$\left(\frac{\rho U h_o}{\eta}\right)_c \approx 1{,}000.$$

This is a conservative estimate. With increasing eccentricities the value tends to increase albeit only very slowly.

By making use of the present concept of a critical or transitional Reynolds number, an attractive simplification of numerical work can be obtained. Indeed, the formula for load-carrying capacity in the case of turbulent flow in the lubricant film can profitably be rewritten as follows:

$$\frac{p_m h_o^2}{\eta U r} = \left(\frac{\rho U h_o}{\eta}\right)^{1+m_o} \left(\frac{\rho U h_o}{\eta}\right)_c^{-(1+m_o)} f_2(\varepsilon, \frac{b}{d})$$

in which the functional relationship $f_2(\varepsilon, \frac{b}{d})$ is known laminar lubrication theory, in which $m_o = -0.25$ for smooth surfaces and in which $\left(\frac{\rho U h_o}{\eta}\right)_c \approx 1{,}000$ for small eccentricities and smooth surfaces, see

appendix 2.

It proves indeed that the above formula roughly agrees with the results of two of the three test series. Excellent agreement can be obtained with Orcutt's experiments, see Fig. 4. In that figure (4a, 4b, 4d and 4e) experimental results are depicted in the manner chosen by Orcutt. Making use of the above formula and of a critical value for the Reynolds number $(\frac{\rho U h_o}{\eta})_c \approx 1{,}000$, leads to a replot of graphs giving the relationship between the inverse of dimensionless load-carrying capacity versus dimensionless eccentricity in Fig. 4c and that between dimensionless frictional torque versus inverse dimensionless load-carrying capacity in the replotted graphs in Fig. 4f. It can be seen in Figs. 4c and 4f that all experimental results can be represented by one line and that this line is close to that for the laminar experimental results. Deviations can be seen to occur only if eccentricity tends to be rather high. Moreover, they are seen to be such as to make the present critical value for the Reynolds number on the conservative side.

1143 Combination of the two main types of flow in parallel directions, curved lubricant film and non-uniform film thickness, both surfaces smooth and ungrooved.

Pan and Vohr (1967) give experimental results pertaining to the above conditions. The bearing tested was a cylindrical fluid film bearing of infinite length; the maximum value of $\frac{\rho U h_o}{\eta}$ was 3,200 and the filmthickness to radius ratio $\frac{h_o}{r} = 0.0104$. It has been demonstrated in the foregoing that in that case we have to do with Taylor vorticity in the lubricant film. Above a given Reynolds number $\frac{\rho U h_o}{\eta}$ the flow becomes fully turbulent and the effect of the curvature only results in an increase of n_o and n_1 in formulae (2) and (3) which may perhaps be neglected for $\frac{h_o}{r} = 0.01$ and $\frac{\rho U h_o}{\eta} > 5{,}000$ (see also sub 1121 and 1122). The test results make it possible to determine the Reynolds number $\frac{\rho U h_o}{\eta}$ for which the effect of vorticity on pressure build-up is negligible. For this purpose, we use those test results

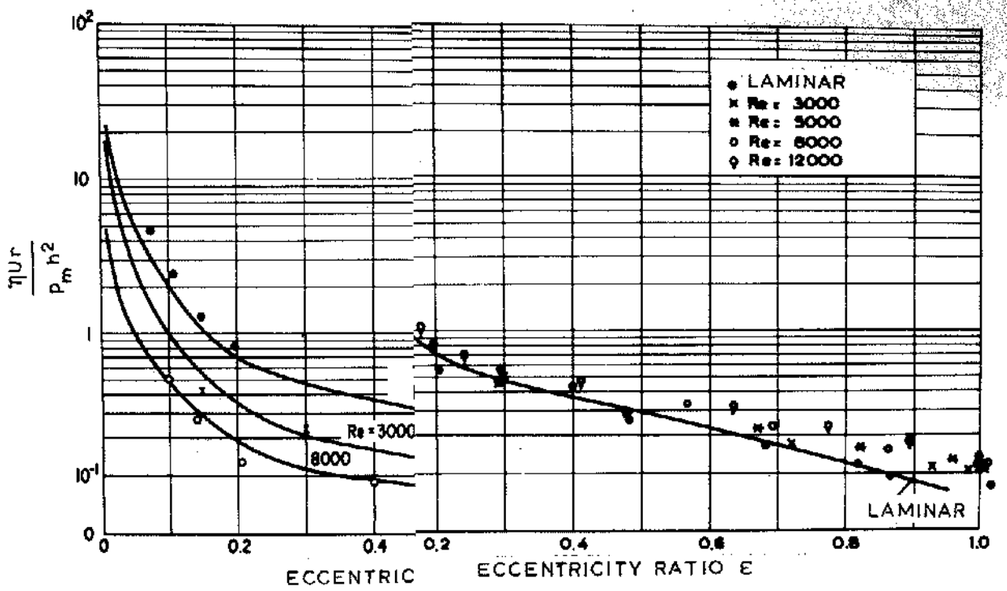

a

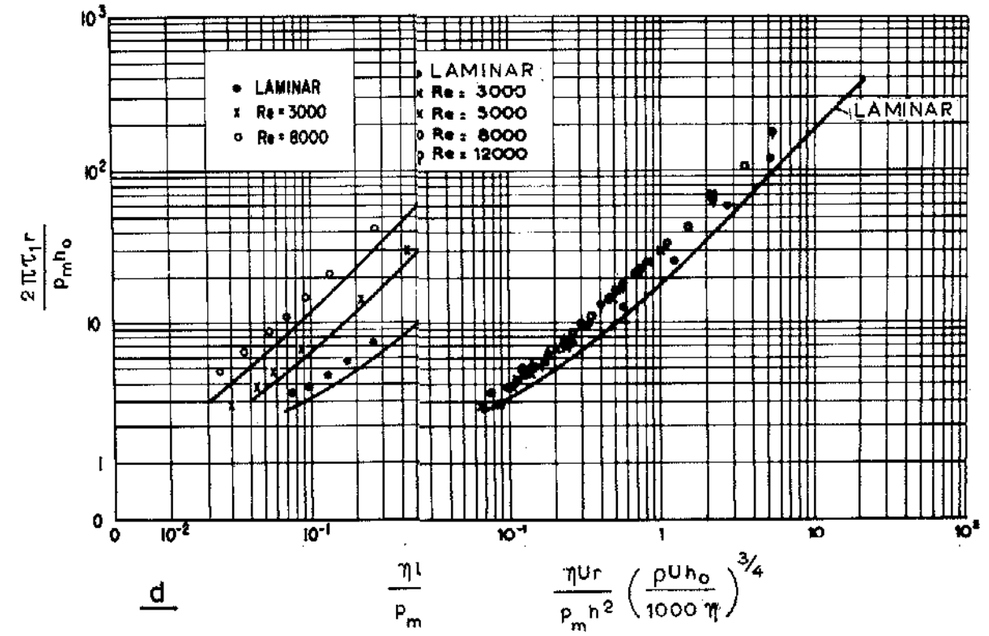

d

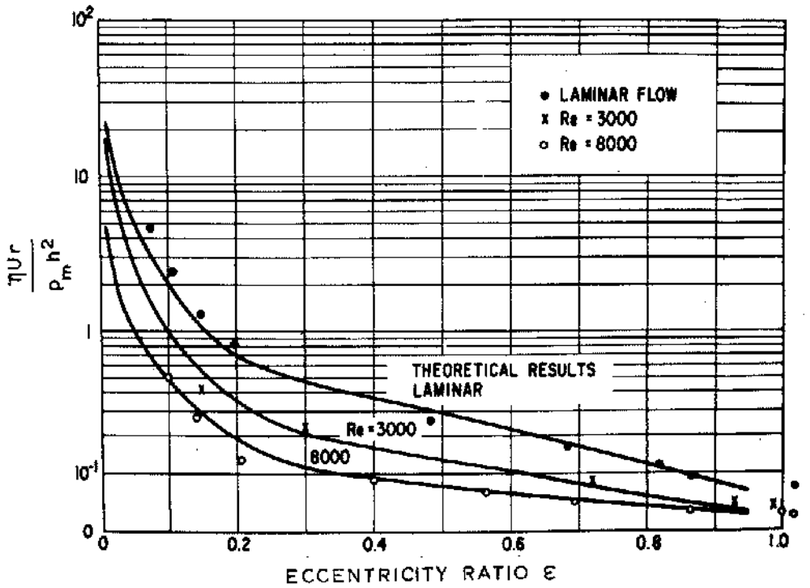

a

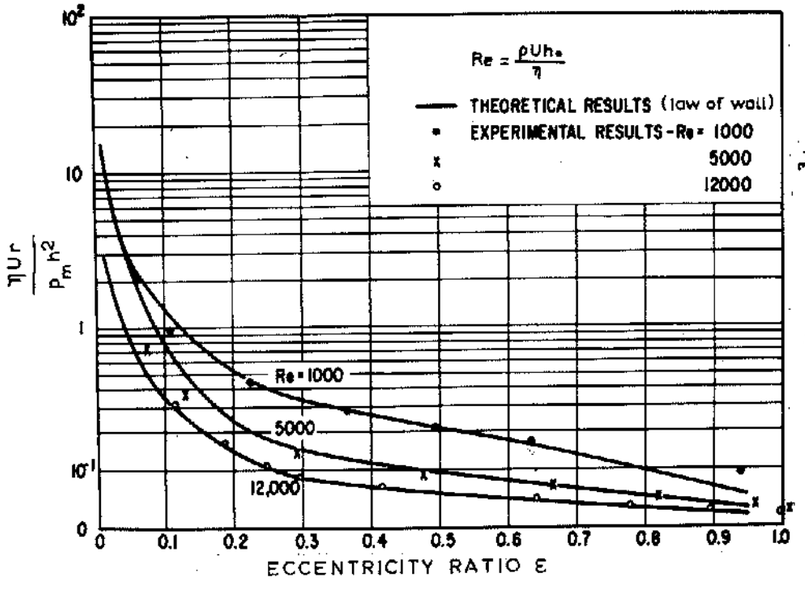

b

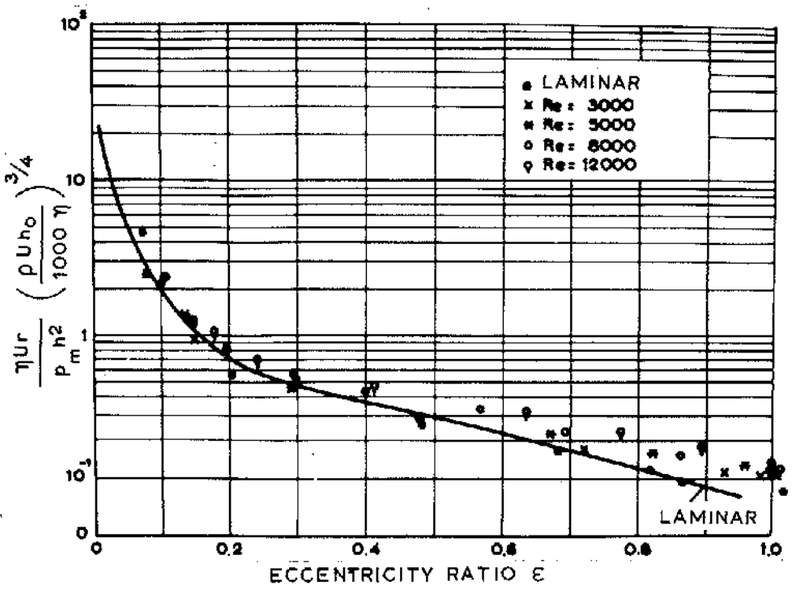

c

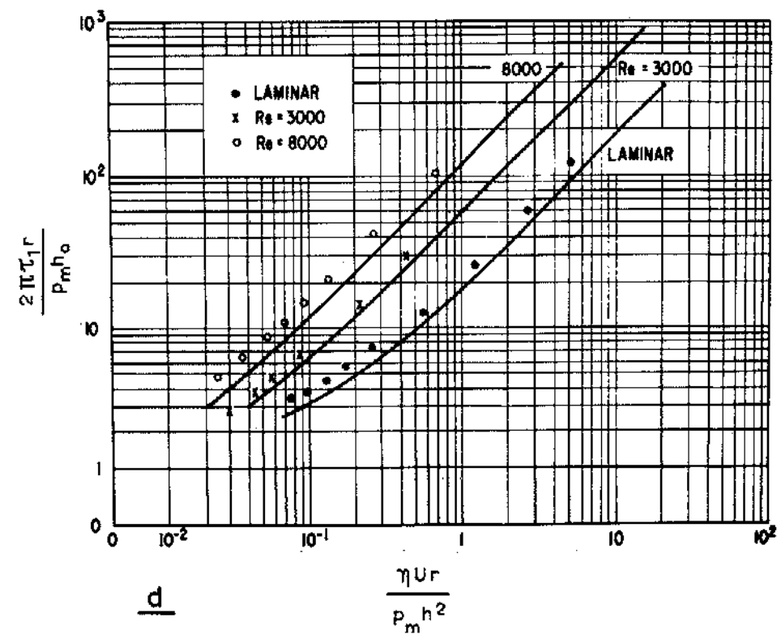

d

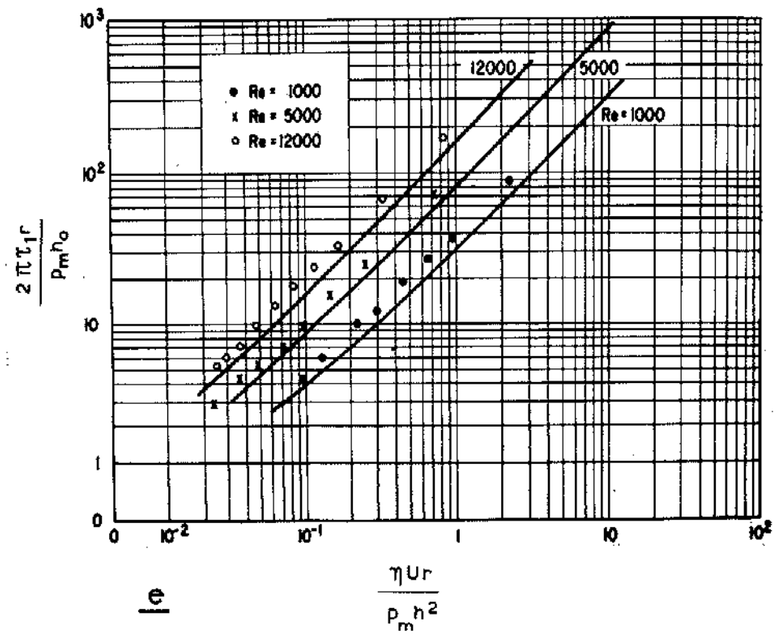

e

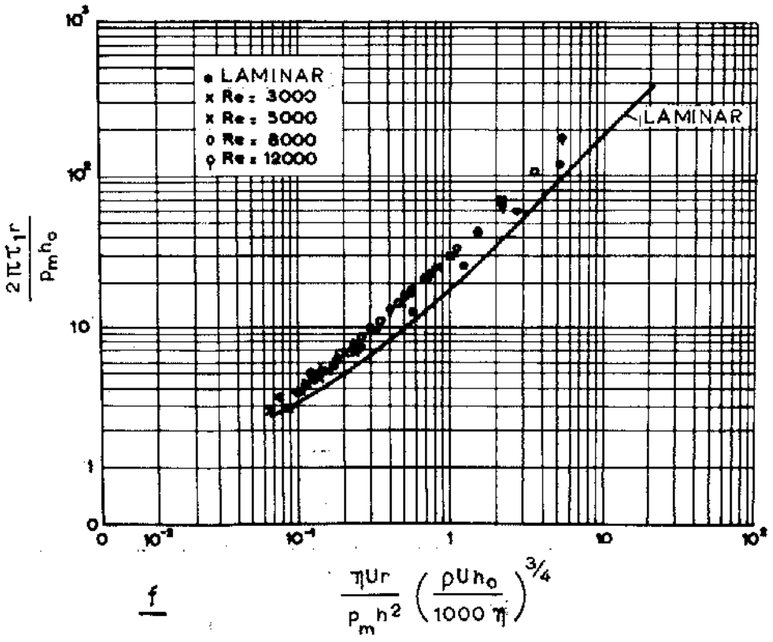

f

Fig. 4 Orcutt's original experimental results for tilting pad bearings (a,b,d and e) and replotted results by the author (c and f)

in which the ratio of the peak pressures in the lubricant film with turbulent and laminair flow is given for Reynolds numbers $\frac{\rho U h_o}{\eta} < 3,200$.

In appendix 2, the author has found the following values for the infinitely wide bearing:

for $\varepsilon = 0.2$

(a) turbulent : $\frac{p_{max} h_o^2}{\eta U r} = 0.007 \left(\frac{\rho U h_o}{\eta}\right)^{3/4}$

(b) laminar : $\frac{p_{max} h_o^2}{\eta U r} = 1.23$

so that:

$$\frac{p_{max\ turbulent}}{p_{max\ laminar}} = 0.0057 \left(\frac{\rho U h_o}{\eta}\right)^{3/4}$$

Comparison of this expression with the experimental results shows that for $\frac{\rho U h_o}{\eta} > 2,400$ there is good agreement and that the estimate on the basis of the theory is less than 10 % lower than the test result.

1311 Pressure flow, plane lubricant film, and uniform film thickness, both surfaces rough and ungrooved.

So far it has been attempted to make the bearing surfaces as smooth as possible. If the flow in the lubricant film is laminar this is no doubt sensible. In that case, roughness of the surfaces has a negligible effect on pressure build-up in and leakage from the lubricant film. Hence roughness would entail that the surfaces would sooner get in contact with each other.

In the case of turbulent flow in the lubricant film it is by no means self-evident that the surfaces should be given a smooth finish. Indeed, it is conceivable that roughness of even a small percentage of the lubricant film thickness may already result in a worthwhile increase in pressure build-up and/or in a reduction of leakage.

From the data compiled by Schlichting (1965) it can be concluded that the constant m_o in the formulae (2), (8a) and (8b) increases with increasing heights of the roughness from a small negative value for smooth surfaces to $m_o = 0$ for very rough surfaces.

It seems possible to achieve an increase in load-carrying capacity of self-acting bearings by a factor of about 2 and a reduction of leakage in externally pressurized bearings by a similar factor 2. It seems that until now, no work pertinent to this improvement of bearing-properties has been published.

2124 Combination of the two main types of flow in directions, including an angle, curved lubricant film, uniform film thickness, both surfaces smooth and grooved.

These conditions are realized in tests by Stair (1967) and Pape (1968) with grooved seals (visco-seals). The seal consists of a shaft with a multiple square screw thread in a smooth bushing; shaft and bushing are accurately concentric, and rotation builds up pressure in axial direction y. In Stair's tests, the shaft rotated in the bushing and vorticity occurred up to certain values of $\frac{\rho Uh}{\eta}$. In Pape's tests the bushing rotated around the shaft and there was a sudden transition from laminar flow to turbulent flow.

From the formulae (8a) and (8b) it can be derived that the following formula would have to be applicable in the turbulent regime:

$$\frac{h^2}{\eta U}\frac{dp}{dy} = n_o\left(\frac{\rho Uh}{\eta}\right)^{1+m_o} \cdot f \text{ (dimensionless groove parameters)},$$

in which $\frac{dp}{dy}$ gives the overall, smoothed axial pressure gradient, h gives the radial clearance. and where f denotes a functional relationship.

Despite the fact that inertia effects must have played a role, Stair's and Pape's tests again give the value $m_o = -0.25$. Hence it appears that this constant never changes as long as $\frac{\rho Uh}{\eta} < 10^5$ and as long as the surfaces are smooth, even though one of them is grooved.

The value of the constant n_o could not be derived from the experiments because the function f of the dimensionless groove parameters has not yet been derived. However, from the experiments it seems possible to derive a critical Reynolds number

$$\left(\frac{\rho Uh}{\eta}\right)_c = n_o f \text{ (dimensionless groove parameters)} \approx 500.$$

The derivation is in the same manner as sub 1134, namely through extrapolating laminar and turbulent flow data.

7. COMPARISON OF THE BULK-FLOW THEORY AND TWO OTHER THEORIES ON THE BASIS OF THE LAW-OF-WALL AND THE MIXING LENGTH CONCEPT.

All equations, that in the various theories give pressure and flow in a turbulent lubricant film, are semi-empirical and contain two empirical constants. The main difference between the bulk-flow theory and the two convential theories, based on the law-of-wall or the mixing-length concept, lies in the choice of the empirical constants. In the first theory, empirical constants are derived from measurements on bulk-flow between stationary or sliding plates and in pipes. In the other two theories, empirical constants are derived from measurements of time-averaged flow velocity profiles between stationary or sliding plates and in pipes. In the first theory it is possible to derive the empirical constants without much insight into the mechanism of turbulent flow. In essence, the author's theory is nothing but a generalization of the well known dependence between friction-factor and Reynolds number that was first given by Blasius (1913). In the other two theories, empirical constants cannot but be derived after having introduced a model of the turbulence mechanism. Indeed, the application of the law-of-wall requires a quantitative determination of the universal velocity profile near a wall and the application of the mixing-length concept requires the determination of the mixing length. However, any model accounting for the turbulence mechanism is only valid for certain limiting conditions. Thus, the validity of such models is a matter of continuing dispute. It is outside the scope of this work to take part in this dispute. Therefore, the practical results of the theory based on the law-of-wall concept, as worked out by Elrod and Ng[1] (1967) and that based on the mixing-length concept, as worked out by Constantinescu (1969)[2], are compared with the author's theory and it will not be discussed at length whether the other investigators have correctly applied realistic, physical models.

In the first place, the three theories must be brought in such

[1] an earlier, linearized, version of this theory was developed by Ng and Pan (1965).

[2] the first publication by Constantinescu on the subject is in Rumanian and dates from 1958.

a form that they can be compared. Practical results of the two conventional theories have been presented by their originators in the form of graphs of the magnitudes G_x en G_y derived from the following two equations that resemble those for plane laminar flow

$$U_x = - G_x \frac{h^2}{\eta U} \frac{\partial p}{\partial x} + \frac{1}{2} \tag{11a}$$

$$U_y = - G_y \frac{h^2}{\eta U} \frac{\partial p}{\partial y} \tag{11b}$$

The first equation gives the dimensionless, mean flow velocity in the direction of sliding. It is seen to consist of a pressure or Poiseuille flow component and a drag or Couette flow component. The second equation (11b) gives the dimensionless, mean pressure flow velocity perpendicular to the direction of sliding. From the graphical results of the two theories, it can be derived that G_x and G_y reach a maximum value of 1/12 for Reynolds numbers smaller than 1000 so that the equations become identical to the equations for laminar flow in that regime. In the turbulent regime G_x and G_y are dependent on the Reynolds number based on sliding speed and local pressure gradient (or Reynolds number based on the local flow velocity due to the local pressure gradient). This feature can be exploited by inserting U_x and U_y (equations 11a and 11b) into equations 8a and 8b. By doing so the bulk flow theory is brought in the same form as the two conventional theories. Indeed, it results in two equations with G_x and G_y as unknowns, and Reynolds number $\frac{\rho U h}{\eta}$ and pressure gradients $\frac{\rho h^3}{\eta^2} \frac{\partial p}{\partial x}$ and $\frac{\rho h^3}{\eta^2} \frac{\partial p}{\partial y}$ as the independent variables. The two equations would appear rather difficult to handle, and therefore are presented here only for two extreme cases. The first case is characterized by $\frac{\partial p}{\partial x} >> \frac{\partial p}{\partial y}$ where x is in the direction of sliding. This condition results in the following two equations:

$$\frac{-\partial P}{\partial X} = \frac{1}{2} n_o \left[\left(-G_x \frac{\partial P}{\partial X} - \frac{1}{2} R \right)^{2+\bar{m}_o} + \left(- G_x \frac{\partial P}{\partial X} + \frac{1}{2} R \right)^{2+m_o} \right] \tag{12a}$$

$$1 = \frac{1}{2} n_o G_y \left[\left(-G_x \frac{\partial P}{\partial X} - \frac{1}{2} R \right)^{1+m_o} + \left(- G_x \frac{\partial P}{\partial X} + \frac{1}{2} R \right)^{1+m_o} \right] \tag{12b}$$

in which $\frac{\partial P}{\partial X} = \frac{\rho h^3}{\eta^2}\frac{\partial p}{\partial x}$; $\frac{\partial P}{\partial Y} = \frac{\rho h^3}{\eta^2}\frac{\partial p}{\partial y}$ en $R = \frac{\rho U h}{\eta}$

The second extreme case is characterized by the condition,

$\frac{\partial p}{\partial y} \gg \frac{\partial p}{\partial x}$, which yields:

$$1 = n_o G_y \left\{G_y^2 \left(\frac{\partial P}{\partial Y}\right)^2 + \frac{1}{4}R^2\right\}^{\frac{1+m_o}{2}} \qquad (13a)$$

$$1 = n_o G_x \left[\left\{G_y^2 \left(\frac{\partial P}{\partial Y}\right)^2 + \frac{1}{4}R^2\right\}^{\frac{1+m_o}{2}} + \frac{1+m_o}{4}R^2\left\{G_y^2\left(\frac{\partial P}{\partial Y}\right)^2 + \frac{1}{4}R^2\right\}^{\frac{-1+m_o}{2}}\right] \qquad (13b)$$

Another extreme case can be distilled from the two sets of equations (12) and (13) by stating that both

$$G_x \frac{\partial P}{\partial X} \text{ and } G_y \frac{\partial P}{\partial Y} \ll \frac{1}{2}R$$

which means that the pressure flow is much smaller than the drag flow. Then it follows:

$$G_x = \frac{2^{1+m_o}}{n_o(2+m_o)} R^{-(1+m_o)} \qquad (14a)$$

$$G_y = \frac{2^{1+m_o}}{n_o} R^{-(1+m_o)} \qquad (14b)$$

in which $n_o = 0.066$ and $m_o = -0.25$ for smooth surfaces and $R < 10^5$, see sub 1111. It is stressed once more that the above two equations are valid only with a dominant drag flow.

By means of the three sets of equations (12) (13) and (14) the bulk-flow theory for turbulent lubricant films has been cast into a form which enables it to be compared with theories based on law-of-wall and mixing-length concept. It is stressed that it proved possible to bring it in closed form and that results of the other two theories do not exist in closed form but have been compiled in graphical form and, when using a computer, in arrays. The main reason is that equations for bulk-flow and pressure build-up can directly be derived

from experiments in the bulk-flow theory and that in the theories based on law-of-wall and mixing-length concept they can be derived only indirectly, i.e. by numerical integration of flow velocity profiles.

Equations based on the bulk-flow theory will now be brought in graphical form and the results depicted in graphs that are derived from the theoretical work by Constantinescu (1969), Ng and Pan (1965), and Elrod and Ng (1967).

In the first place some attention will be given to the case that pressure flow is much smaller than drag flow (equations (14a) and (14b)). Graphical results are presented in Figs. 5a and 5b.[1] Red lines are results from the bulk flow theory. Drawn black lines are results from the law-of-wall (Ng and Pan) and dotted black lines are based on the mixing-length concept (Constantinescu). It can be seen that the dependency between G_x and $R = \frac{\rho U h}{\eta}$ is rougly identical for the three theories in a regime characterized by $10^4 < R < 10^5$. However, theoretical results from the mixing-length theory can be brought into accordance with the other two theories only by suitably modifying the mixing-length constant k^x. Thus, from the comparison in a regime characterized by $10^4 < R < 10^5$ as far as G_x is concerned, it follows that Constantinescu's mixing-length theory is less reliable than the other two theories. This feature is even more apparent from the comparison of values for G_y in the same regime. Values derived from the bulk flow theory and Ng and Pan's law-of-wall theory are reasonably close. However, values derived from the mixing-length theory show a rather great deviation and cannot be regarded to give an accurate prediction of the actual values in lubricant films. Thus, predicted values for G_y are less accurate than those for G_x in Constantinescu's mixing-length theory. This is probably not due to inadequacies of the mixing-length concept as a physical model, but to ignoring the vectorial character that here has to be assigned to Prandtl's mixing-length concept[2]. By correctly applying the mixing-

[1]) derived from Constantinescu's Fig. 6.14, and Ng and Pan's Fig. 18.

[2]) Pages 45, 74 and 282 in Constantinescu's book of 1969 give expressions for the turbulent stress based on the mixing-length concept. The last expression 6.12 reflects its vectorial character but has not been used. This can be shown to weigh most heavily as regards the values for G_y.

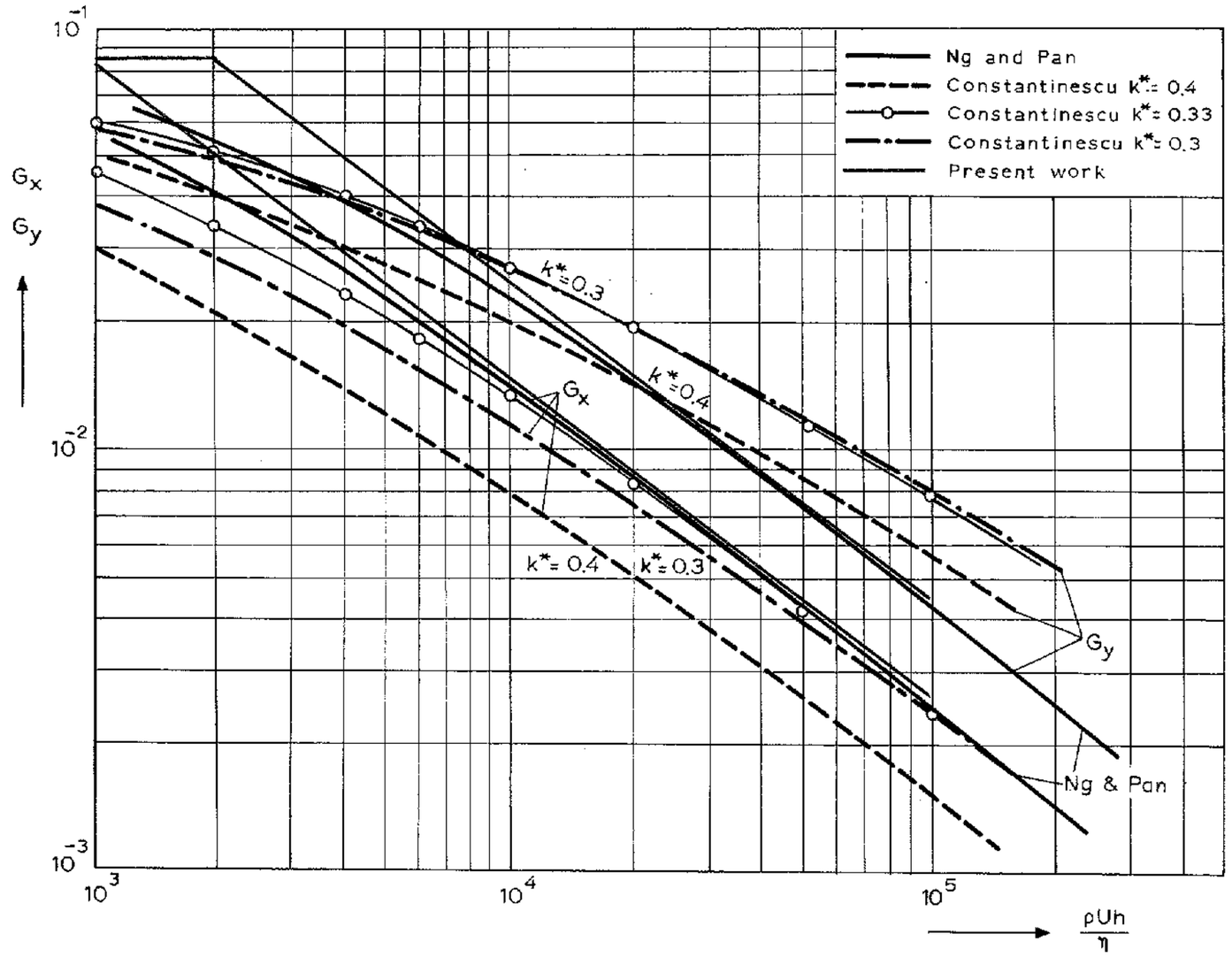

Fig. 5a Variation of G_x and G_y with $\frac{\rho U h}{\eta}$ if drag flow is dominant.

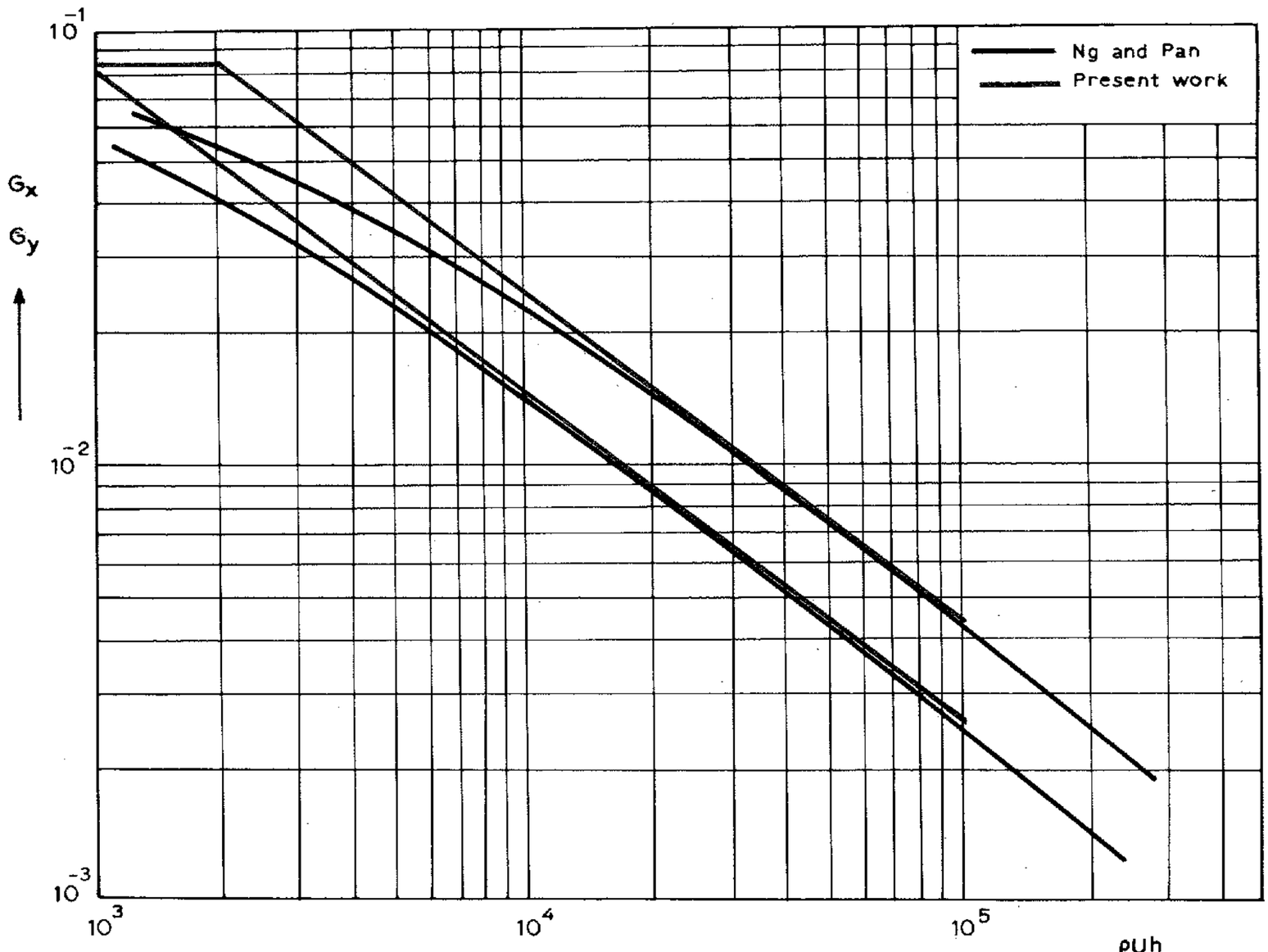

Fig. 5b Variation of G_x and G_y with $\frac{\rho U h}{\eta}$ if drag flow is dominant.

length concept and duly accounting for its vectorial character, values for G_y could be made to come equally close to values for G_y derived from the other two theories as is the case for G_x. One major drawback of the mixing-length approach remains unshattered in that values for both G_x and G_y can be brought into accordance with the other two theories only by modifying or adapting the empirical constant k^x, see Fig. 5. Thus, the mixing-length approach stands out as the least reliable of the three methods in discussion.

The above discussion makes it plausible that the mixing-length approach may just as well be left out of the comparison. Then, only the discrepancies between the law-of-wall theory and the bulk flow theory in a regime characterized by $\frac{\rho U h_o}{\eta} < 10^4$ still remain to be explained. This explanation will be part of the following, more general comparison between bulk flow theory and law-of-wall theory.

An extra reason for leaving the mixing-length theory out of the following comparison is the fact that this theory has not been worked out for the general cases in which drag flow may well be as great as or smaller than pressure flow. Such general cases occur in hybrid and externally pressurized bearings where drag flow need not be dominant as in the previous cases.

A search for a general treatment of the turbulent lubricant film exclusively produced Elrod and Ng, i.e. in the form of their work based on the law-of-wall concept. In their paper, they show that Ng and Pan's linearized theory is in accordance with their general theory. The comparison between bulk flow theory and their law-of-wall theory takes place by inserting numerical values for G_x and G_y derived from equations (12a) (12b) (13a) and (13b) in graphs first published by Elrod and Ng, see Figs 6 and 7[1]. In these figures, values for G_x and G_y derived from eqs. (11a) and (11b) are plotted for several values of the dimensionless pressure gradient and with Reynolds number based on sliding speed as the independent variable. In these figures, red lines are results from the bulk flow theory and black lines are results from the law-of-wall theory. Drawn lines represent cases in which pressure gradient and direction of sliding are roughly

[1]) These graphs are based on numerical work presented in appendix 3.

perpendicular, so that $\frac{\partial p}{\partial y} \gg \frac{\partial p}{\partial x}$. Dotted lines represent cases in which pressure gradient and sliding speed are almost parallel or $\frac{\partial p}{\partial x} \gg \frac{\partial p}{\partial y}$. It can be deduced from the two figures that it is unimportant how the pressure gradient and sliding speed are directed with respect to each other for $R \to \infty$ and $R \to 0$, the former cases being representative of a dominant flow due to a sliding surface, and the latter of a dominant flow under the influence of a pressure gradient. In such cases, the drawn and the dotted lines can be seen to coincide. The drawn and the dotted lines deviate in a regime where the two flow components have the same order of magnitude. From a comparison between the red lines representing bulk flow theory and the black lines representing law-of-wall theory, it follows that the two theories show the general behaviour outlined above and, also, that they are in accordance.

A comparison between the red and the corresponding black lines also shows that discrepancies are present for the smaller Reynolds numbers ($R < 10^4$) and for the smaller dimensionless pressure gradients. Indeed, the accordance is excellent in Fig. 6 and not so good in Fig.7. Such increasing discrepancies for decreasing Reynolds numbers can also be seen in Fig. 5, which is representative of a dominant drag flow.

It remains to be explained why the two theories agree well only over part of the turbulent regime covered, and which is the better one in the remaining part of this regime. The explanation can be found in Elrod's and Ng's own work, see Fig. 8. In this figure black dotted lines are based on their law-of-wall theory and black and red drawn lines are the result of experiments used by them and the author, respectively. The vertical co-ordinate gives the friction factor

$$\frac{2\tau}{\rho u_m^2} \text{ or } \frac{8\tau}{\rho U^2} \text{ and}$$

the horizontal gives the Reynolds number

$$\frac{2\rho u_m h}{\eta} \text{ or } \frac{\rho U h}{\eta}.$$

Elrod and Ng chose this way of plotting theoretical and experimental results in order to be able to compare in one single graph drag flow,

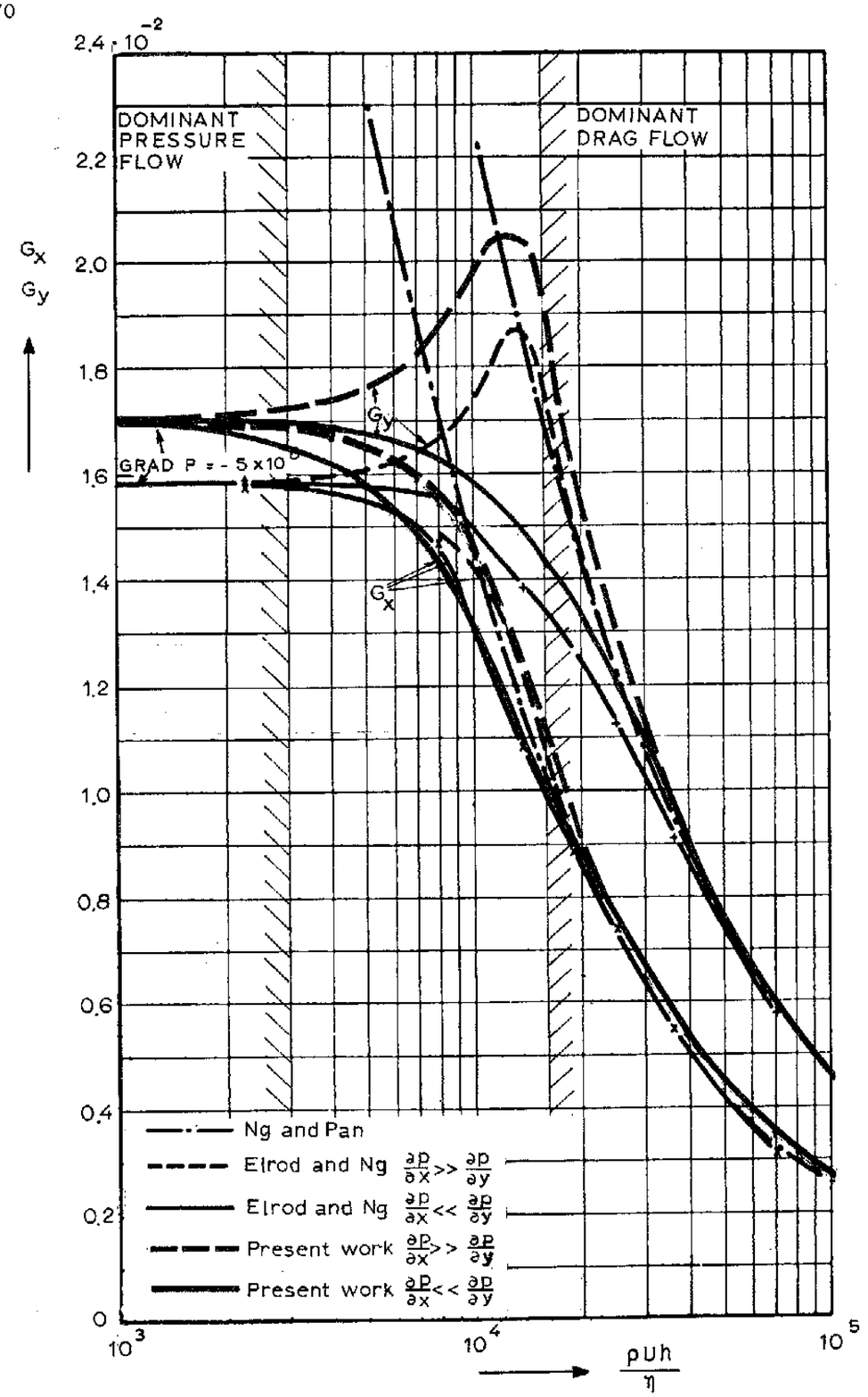

Fig.6 Variations of G_x and G_y with $\frac{\rho U h}{\eta}$ at a great pressure gradient.

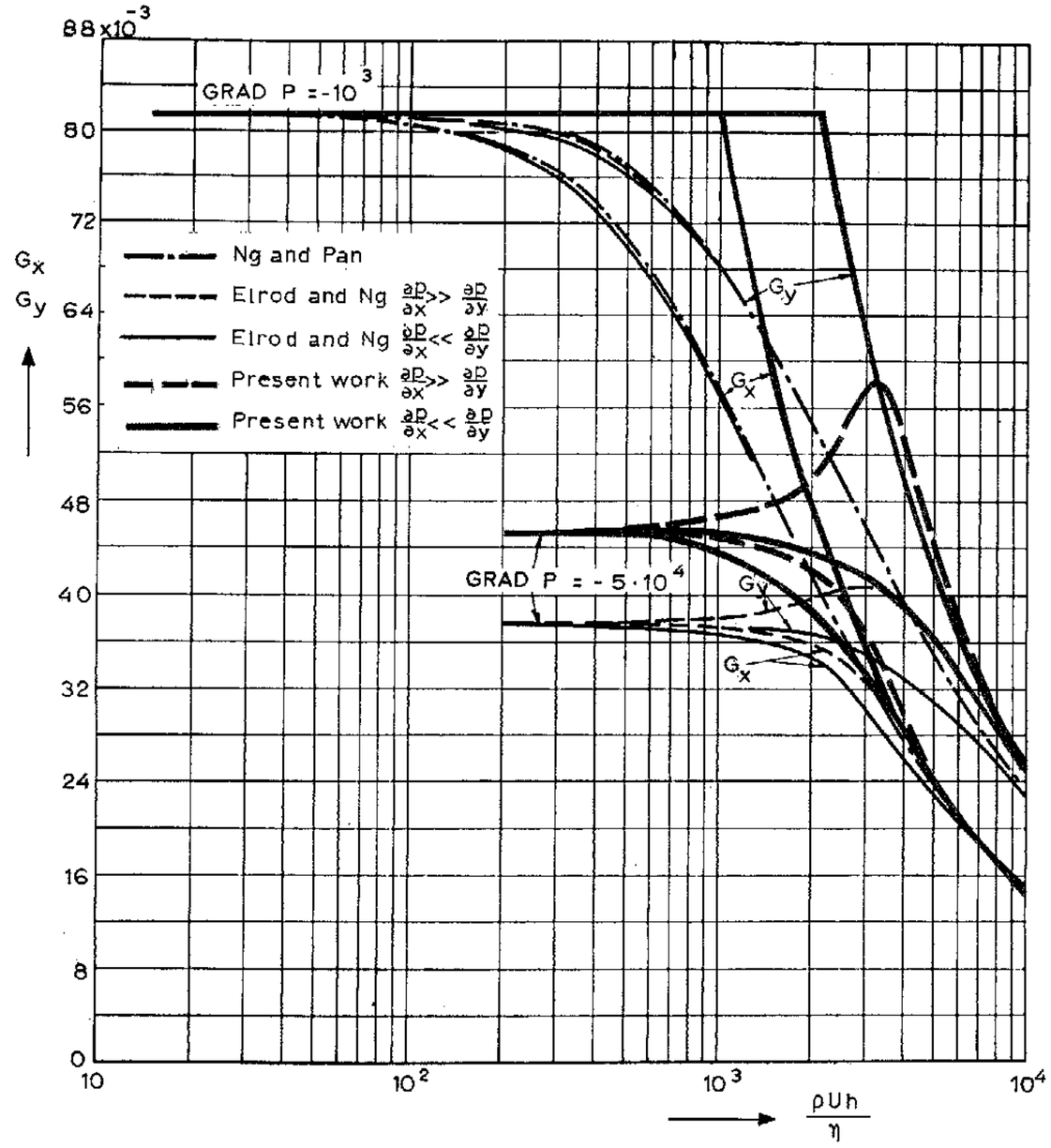

Fig. 7 Variation of G_x and G_y with $\frac{\rho U h}{\eta}$ at two small pressure gradients.

due to sliding of a surface, with pressure flow, under the influence of a pressure gradient. When discussing this figure Elrod and Ng state that the law-of-wall theory is asymptotically correct in the limits of high and low Reynolds numbers and that it is not to be expected offhand, that any agreement can be achieved in the transition region which extends up to $\frac{\rho U h}{\eta} = 10^4$.

Indeed, it follows from Fig. 8 that a theory based on law-of-wall does not agree so well with experiments as the bulk-flow theory, which is based directly on experiments. But the lack of agreement is restricted to the smaller Reynolds numbers, the situation being much better at sufficiently high such numbers.

The general conclusion is that the bulk-flow theory emerges as the most reliable one of the three theories that have been compared in this section.

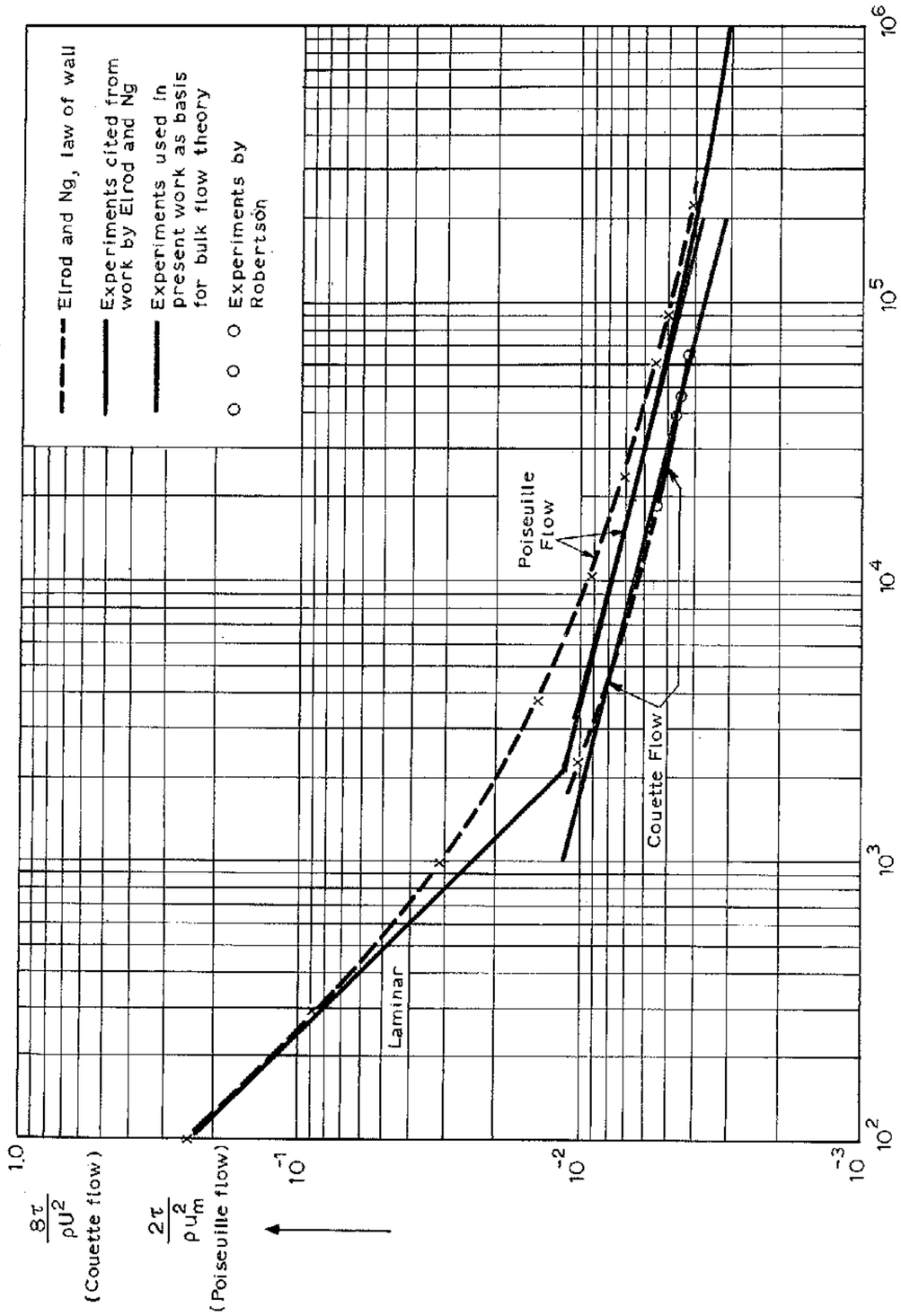

Fig. 8 Variations of friction factors with Reynolds numbers.

8. DESIGN DIRECTIVES FOR TURBULENT SELF-ACTING FLUID FILM BEARINGS

The bulk-flow theory outlined in this thesis as well as the other two theories have not been completely worked out numerically. The numerically most complete piece of information is that by Orcutt (1967) on the tilting pad bearing. His design data on the tilting pad bearing are based on the law-of-wall theory and are amply sufficient for designing. For other bearings, however, such design data are not yet available, at least none that are based on sound theory for turbulent fluid films.

The bulk-flow theory has so far been worked out numerically but to a limited extent, i.e. only as regards the load-carrying capacity of an infinitely wide, plain journal bearing.[1]) However, the theory will be shown to be applicable, at least in principle, to the design of all other types of turbulent, self-acting fluid film bearings.

In chapter 6 sub 1134, the concept of the critical Reynolds number has been introduced. The value for this Reynolds number indicates the transition from laminar to turbulent flow in so far as it affects pressure build-up in the lubricant and the load-carrying capacity. This critical number is a poor indication of the actual transition from laminar to turbulent flow in the film, this transition being not sharp but covering a rather wide regime of Reynolds numbers. That is, through extrapolating computed load-carrying capacities of a bearing operating in the laminar regime and in the turbulent regime, a critical Reynolds number could be determined yielding equal "laminar" and "turbulent" load-carrying capacities. In appendix 2 and in chapter 6 sub 1134, it has been shown that the value for such a critical Reynolds number for plain journal bearings of great width amounts to about 1,000 ($(\frac{\rho U h_o}{\eta})_c \approx 1{,}000$). Excellent agreement could be shown to exist between this prediction and the value which could be derived from Orcutt's experiments on a tilting-pad bearing up to eccentricities $\varepsilon < 0.5$. As expected, the value of this number appears to be in-

[1]) Appendix 2.

sensitive to the type of bearing and to the eccentricity at which it operates. The same value for the critical Reynolds number can be derived by equating laminar and turbulent values for G_x in equations (11a) and (14a).

However, it can be shown that at very great eccentricities and with the smaller width-diameter ratios the critical Reynolds number tends to be greater than 1,000 albeit only moderately so. From experiments by Pape (1968) it follows that for grooved bearings the critical Reynolds number based on radial clearance is smaller than 1,000. This is due to the fact that turbulence can be created in the grooves while flow on ridges is still laminar.

After having estimated the critical Reynolds number, the design of self-acting bearings may proceed along the following lines:

1. Calculate the bearing as if the flow is laminar:

   $$\frac{p_m h_o^2}{\eta U r} = f \text{ (eccentricity and design parameters)}$$

   where f is a functional relationship that may be found in textbooks on laminar film bearings.

2. Estimate the Reynolds number

   $$\frac{\rho U h_o}{\eta}$$

   If the Reynolds number is smaller than the critical one (1,000), the calculation sub 1 is complete.

3. If the Reynolds number is greater than the critical one, calculate the bearing as if the flow is turbulent. Do this with help of the following formula, which was derived in chapter 6 sub 1134, viz.:

   $$\frac{p_m h_o^2}{\eta U r} = \left(\frac{\rho U h_o}{\eta}\right)^{1+m_o} \left(\frac{\rho U h_o}{\eta}\right)_{cr}^{-(1+m_o)} f \text{ (eccentricity and design parameters)}$$

   Note that $(\frac{\rho U h_o}{\eta})_c \approx 1{,}000$ in the majority of practical cases and $m_o = -0.25$ for smooth surfaces.

4. Verify whether inertia effects other than those inherent in turbulence are negligible. Do this by means of the dimensionless parameter α, as defined by expression (10c), checking whether indeed: $\alpha < 0.5$.

where $\alpha = \frac{h_o}{d} \frac{1}{n_o} \left(\frac{\eta}{\rho U h_o}\right)^{m_o}$

in which $n_o = 0.066$ and $m_o = -0.25$.

5. Diminish clearances if load-carrying capacity is too low or inertia effects are excessive.

No such simple design directives have so far been derived for externally pressurized bearings and hybrid bearings. For such cases the full (differential) equations based on bulk-flow theory or law-of-wall theory have to be solved for the pressure build-up. However, for these cases design information is not completely lacking. Indeed, experimental results from Roberts and Bett's (1969), Yamada's (1962), Decker's (1965) work are available. Further results of theoretical and experimental work by the author on externally pressurized and hybrid bearings will be published in due course.

9. ACKNOWLEDGEMENTS

The present work on turbulent lubricant films was carried out at the Institute TNO for Mechanical Constructions, whilst several employees co-operated with the author. It was sponsored by the Association Euratom - TNO/RCN as part of the Sodium Technology Development Programme [1] and administered by A.H. de Haas van Dorsser. When developing the theory advice was given by R.A. Burton, at the time, at the U.S. Office of Naval Research, London, Professor J.O. Hinze, University of Technology, Delft, and A. Verduin, Central Technical Institute TNO, Apeldoorn. Results of this work have meanwhile been used for testing and designing bearings for Stork liquid-sodium pumps, now running successfully. In the course of this particular work, close co-operation was achieved with G.A. Bos in the initial stage and later with E.J. Bussemaker, both from Stork, Hengelo, and also with R.H. Fakkel, Neratoom, Den Haag.

[1] Contract No. 013 - 65 - 1 RAA N;
Turbulent lubricant film. Special Report - TN/6701 - 08,
Jan. 1967;
The turbulent lubricant film: A comparison of theoretical and experimental results, Special Report - TN/6801 - 16,
Jan. 1968;
available from Organisation for Industrial Research TNO, Holland, subject to approval of the relevant authorities.

10. LIST OF REFERENCES

Blasius H. — Das Ähnlichkeitsgesetz bei Reibungsvorgängen in Flüssigkeiten. Forschg. Arb. Ing.-Wes., Heft 131, Berlin (1913).

Burton R.A. — On the close relationships between turbulent plane-Couette and pressure flows, J. Aerospace Sci, vol 29, p 1004 (1962).

Burton R.A. Y.C. Hsu. — Fundamental investigation of liquid-metal lubricated journal bearings. Second topical report SwRI - 1228 P8-32 Final report SwRI - 1228 P8-30 Southwest Research Institute, San Antonio, Texas (1967).

Carper H.J. J.U. Heilhecker, E. Logan. — The effect of a change in wall roughness on turbulence intensity and shear-stress distribution in a two-dimensional channel flow. 8th Midwestern Mechanics Conference, Case Institute of Technology (1963).

Constantinescu V.N. — Lubrication in turbulent regime, transl. by R.A. Burton, U.S. Atomic Energy Commission Division of Technical Information, AEC-tr-6959, avail. Clearinghouse for Federal Scientific and Technical Information, Springfield, Virginia 22151.

Constantinescu V.N. — On the pressure equation for turbulent lubrication, Discussion to Session 2, Fluid film lubrication of the Conference on Lubrication and Wear, London, 1967, Institution of Mechanical Engineers.

Couette M. — Etudes sur le frottement des liquides, Ann. Chem. Phys., vol. 21, no. 6 (1890).

Duffin S. B.T. Johnson. — "Some experience and theoretical studies of journal bearings for large turbo-generator sets", Symposium on Lubrication and Wear 1966 (Sept.), Paper 4, Instn Mech. Engrs, London.

Davies S.J. C.M. White. — An experimental study of the flow of water in pipes of rectangular section. Proc. Roy. Soc. A 119,92 (1928)

Decker O. G.E. Shimp. — Mercury-lubricated hybrid bearing for the Silent Compact Auxiliary Power System. ASLE Trans, vol. 8, no. 4, p.357 (1965).

Elrod H.G. C.W. Ng. — A theory for turbulent films and its application to bearings. J. of Lubr. Techn., ASME Trans., vol. 89, series F, no. 3 (1967).

Hartnett J.P. J.C.Y. Koh, S.T. McComas. — A comparison of predicted and measured friction factors for turbulent flow through rectangular ducts. Trans. ASME, ser. C.J. Heat Trans., vol 84, no 2 1962.

Hirs G.G. — Load Capacity and Stability Characteristics of Hydrodynamic Grooved Journal Bearings , Transactions of the American Society of Lubrication Engineers, Vol. 8, No. 3, July 1965.

Hirs G.G. — Partly Grooved, Externally Pressurized Bearings , Paper 21, Lubrication and Wear Convention 1966, Scheveningen, Holland, Institute of Mechanical Engineers, London.

Ito H. — Friction factors in turbulent flow in curved pipes, J. of Basic Eng., ASME Trans., vol. 81, series D (1959).

Ketola H.W. J.D. Mc Hugh. — Experimental investigation of water lubricated bearings in the turbulent regime, in Bearing and Seal Design in Nuclear Power Machinery, ed. R.A. Burton, ASME, New York, N.Y. (1967).

Koch R. R. Feind. — Druckverlust und Wärme-übergang in Ringspalten, Chemie-Ing. Techn., vol. 30 (1958).

Laufer J. — The structure of turbulence in full-developed pipe flow, NACA Tech. Report 1174 (1954).

Ng C.W. C.H.T. Pan. — A linearized turbulent lubrication theory ASME Trans., J. of Basic Eng., vol. 87, nr 3 (1965).

Orcutt F.R. — The steady-state and dynamic characteristics of the tilting-pad journal bearing in laminar and turbulent flow regimes, J. of Lubr. Tech., ASME Trans, vol. 89, series F, no 3 (1967)

Pape J.G. W.J. Vrakking. — Viscoseal-Pressure Generation and Friction Loss under Turbulent Conditions , ASLE Trans. Vol. 11, no 1 (1968)

Pan C.H.T., J. Vohr. — Super-laminar flow in bearings and seals, in Bearing and Seal Design in Nuclear Power Machinery, ed. R.A. Burton, ASME, New York, N.Y. (1967).

Prandtl L. — Über die ausgebildete Turbulenz, ZAMM, vol. 5 (1925).

Reichardt H. — On the velocity distribution in a rectilinear turbulent Couette flow, ZAMM, special supplement (1956).

Robertson J.M. — On turbulent plane-Couette flow, in 6th Midwestern Conference on Fluid Mechanics, The University of Texas, Austin (1959).

Schlichting H. — Grenzschicht - Theorie
G. Braun, Karlsruhe (1965).

Shinkle J.W.. K.G. Hornung. — Frictional characteristics of liquid hydrostatic journal bearings,
J. of Basic Eng., ASME Trans., series D, vol. 87 (1965).

Smith M.I. D.D. Fuller. — Journal bearing operating at super-laminar speeds, ASME Trans, vol. 78 (1956).

Stair W.K. R.H. Hale. — The turbulent visco-seal-theory and experiment, Paper H2, 3rd International Conference on Fluid Sealing, B.H.R.A., Cranfield, Bedford (1967).

Tao L.W. W.F. Donovan. — Through-flow in concentric and eccentric annuli of fine clearance with and without relative motion of the boundaries,
ASME Trans., vol. 77, November (1955).

Tao L.W. — A theory of lubrication with turbulent flow and its application to slider bearings,
J. Appl. Mech., vol. 27, no 1 (1960).

Taylor G.I. — Stability of a viscous liquid contained between two rotating cylinders,
Phil. Trans. A 233 (1923).

Voorhees J.E. R.H. Prause, H.C. Meacham. — The design and evaluation of a super-critical speed helicopter power-transmission shaft,
J. of Eng. f. Ind., ASME Trans., vol. 84, series B, no 4 (1967).

White C.M. — Fluid friction and its relation to heat transfer.
Trans. Inst. Chem. Eng., vol. 10 (1932).

Yamada Y. — Resistance of a flow through an annulus with an inner rotating cylinder,
Bull. of JSME, vol. 5, no 18 (1962).

11. LIST OF SYMBOLS

a	constant, index indicating stationary surface
b	bearing width, index indicating sliding surface
d	diameter
e	eccentricity
f (..)	functional relationship
G_x G_y	constants defined in equations (11a) and (11b)
h	film thickness
h_o	radial clearance
m; m_o; m_1	constants, see formulae (1), (2) and (3)
n; n_o; n_1	constants, see formulae (1), (2) and (3)
p	pressure
p_1	fictitious pressure
p_m	mean pressure per unit projected bearing area
p_r	representative pressure
Q_x, Q_y	volumetric flow rate per unit of width
Re	Reynolds number based on characteristic velocity
r_1	pipe radius
r	radius of curvature, radius of cylindrical bearing, index indicating representative pressure
U	sliding velocity
u_m	mean velocity of flow relative to stationary surface
u_x	mean velocity in x direction
u_y	mean velocity in y direction
$U_x = \frac{u_x}{U}$	dimensionless mean velocity of flow in x direction
$U_x = \frac{u_y}{U}$	dimensionless mean velocity of flow in y direction

x, y: co-ordinates in sliding direction and at right angles to sliding direction in the plane of and attached to the stationary surface

z: co-ordinate perpendicular to x and y

$\underline{x}$, $\underline{y}$: co-ordinates in sliding direction and at right angles to the sliding direction in the plane of and attached to the body of the lubricant film (wedge)

τ: shear stress at a surface

τ_o: ditto due to flow under the influence of a pressure gradient

τ_1: ditto due to the sliding of a surface

ρ: density

η: viscosity

$\varepsilon = \frac{e}{r}$: dimensionless eccentricity

$\frac{\partial P}{\partial X} = \frac{\rho h^3}{\eta^2} \frac{\partial p}{\partial x}$: dimensionless pressure gradient

$\frac{\partial P}{\partial Y} = \frac{\rho h^3}{\eta^2} \frac{\partial p}{\partial y}$: dimensionless pressure gradient

$\text{GRAD } P = \left\{\left(\frac{\partial P}{\partial X}\right)^2 + \left(\frac{\partial P}{\partial Y}\right)^2\right\}^{\frac{1}{2}}$: resultant dimensionless pressure gradient

$R = \frac{\rho U h}{\eta}$: Reynolds number based on sliding speed

APPENDIX 1

This appendix is devoted to formulating equations (8a) and (8b) differently. It is characteristic of the formulation in these equations that pressure gradients are explicit and that flow velocities are implicit in the equations. When applying the continuity condition it is useful to have at one's disposal equations in which pressure gradients are implicit and flow velocities are explicit. Such equations can be derived from equations (7a) - (7d). However, it is impossible to eliminate the fictitious pressure gradient. The resulting equations are:

$$U_x = -n_o^{-\frac{1}{2+m_o}} \frac{\left(\frac{h^2}{\eta U} \frac{\partial(p+p_1)}{\partial x} \left(\frac{\eta}{\rho U h}\right)\right)^{\frac{1+m_o}{2+m_o}}}{\left[\left\{\frac{h^2}{\eta U} \frac{\partial(p+p_1)}{\partial x}\right\}^2 + \left\{\frac{h^2}{\eta U} \frac{\partial(p+p_1)}{\partial y}\right\}^2\right]^{\frac{1+m_o}{2(2+m_o)}}}$$

$$= -n_o^{-\frac{1}{2+m_o}} \frac{\left(\frac{h^2}{\eta U} \frac{\partial(p-p_1)}{\partial x} \left(\frac{\eta}{\rho U h}\right)\right)^{\frac{1+m_o}{2+m_o}}}{\left[\left\{\frac{h^2}{\eta U} \frac{\partial(p-p_1)}{\partial x}\right\}^2 + \left\{\frac{h^2}{\eta U} \frac{\partial(p-p_1)}{\partial y}\right\}^2\right]^{\frac{1+m_o}{2(2+m_o)}}} + 1$$

$$U_y = -n_o^{-\frac{1}{2+m_o}} \frac{\left(\frac{h^2}{\eta U} \frac{\partial(p+p_1)}{\partial y} \left(\frac{\eta}{\rho U h}\right)\right)^{\frac{1+m_o}{2+m_o}}}{\left[\left\{\frac{h^2}{\eta U} \frac{\partial(p+p_1)}{\partial x}\right\}^2 + \left\{\frac{h^2}{\eta U} \frac{\partial(p+p_1)}{\partial y}\right\}^2\right]^{\frac{1+m_o}{2(2+m_o)}}}$$

$$= -n_o^{-\frac{1}{2+m_o}} \frac{\left[\frac{h^2}{\eta U}\frac{\partial(p-p_l)}{\partial y}\left(\frac{\eta}{\rho U h}\right)\right]^{\frac{1+m_o}{2+m_o}}}{\left[\left\{\frac{h^2}{\eta U}\frac{\partial(p-p_l)}{\partial x}\right\}^2+\left\{\frac{h^2}{\eta U}\frac{\partial(p-p_l)}{\partial y}\right\}^2\right]^{\frac{1+m_o}{2(2+m_o)}}}$$

Thus, two equations emerge for each of the dimensionless flow velocities U_x and U_y. The elimination of the fictitious pressure gradients, which seems to be rather complicated, would lead to one equation for U_x and one for U_y. These two equations can be inserted into the equation of continuity.

APPENDIX 2

In this appendix a solution of equation (8a) is presented for a film profile represented by $h = h_o(1+\varepsilon\cos\varphi)$, which is typical of journal bearings. This solution is worked out for $\varepsilon = 0.2$ and $p=0$ at $\varphi_{min} = 0$, whilst $p=0$ also at $\varphi_{max} = 180^\circ$. Substitutions are, $x = \varphi r$; $U_y = 0$; $Q_x = U_x \frac{h}{h_o}$ = constant; $n_o = 0.066$; $m_o = -0.25$.

First a table is organized as follows:

ε	Q_x		
$\frac{ph_o^2}{\eta U r}\left(\frac{\eta}{\rho U h_o}\right)^{0.75}$	from 0° until 180° step 1°		
0-45°	45°-90°	90°-135°	135°-180°
$\frac{p_m \sin\beta h_o^2}{\eta U r}\left(\frac{\eta}{\rho U h_o}\right)^{0.75}$	$\frac{p_m \cos\beta h_o^2}{\eta U r}\left(\frac{\eta}{\rho U h_o}\right)^{0.75}$	$\frac{p_a h_o^2}{\eta U r}\left(\frac{\eta}{\rho U h_o}\right)^{0.75}$	
$\frac{p_m h_o^2}{\eta U r}\left(\frac{\eta}{\rho U h_o}\right)^{0.75}$	$\tan\beta$		

Then, for the prescribed value of ε (and Q_x), the values for all the other expressions and quantities are evaluated, and the table is filled out. The maximum value of

$$\frac{ph_o^2}{\eta U r}\left(\frac{\eta}{\rho U h_o}\right)^{0.75} = 0.07$$

is underlined, see next table.

No results of a solution of an equation for laminar flow are given here. Suffice it here to give the maximum value of $\frac{ph_o^2}{\eta U r}$:

$$\frac{p_{max} h_o^2}{\eta U r} = 1.23$$

and also the value of the dimensionless group for the load-carrying

capacity $\frac{p_m h_o^2}{\eta U r} \cong 0.97$ corresponding with the above-specified particular case.

By equating $\frac{p_m h_o^2}{\eta U r}$ and $\frac{p_m h_o^2}{\eta U r}(\frac{\eta}{\rho U h_o})^{0.75}$

a critical Reynolds number can be found for which laminar and turbulent films yield equal load-carrying capacity, viz.,

$$(\frac{\rho U h_o}{\eta})_c \cong 1.000.$$

The value of this critical Reynolds number has been used in chapter 6 sub 1134 and in chapter 8.

.200000/ 00	.477649/ 00		
.874580/-04	.423816/-02	.685427/-02	.565706/-02
.174906/-03	.431179/-02	.687607/-02	.558041/-02
.262336/-03	.438482/-02	.689629/-02	.550167/-02
.349737/-03	.445725/-02	.691493/-02	.542085/-02
.437100/-03	.452906/-02	.693196/-02	.533797/-02
.524415/-03	.460023/-02	.694735/-02	.525305/-02
.611673/-03	.467075/-02	.696109/-02	.516609/-02
.698864/-03	.474060/-02	.697314/-02	.507712/-02
.785979/-03	.480977/-02	.698350/-02	.498617/-02
.873007/-03	.487823/-02	.699214/-02	.489325/-02
.959940/-03	.494598/-02	.699904/-02	.479838/-02
.104677/-02	.501300/-02	.700417/-02	.470159/-02
.113348/-02	.507926/-02	.700752/-02	.460292/-02
.122007/-02	.514475/-02	.700907/-02	.450237/-02
.130652/-02	.520946/-02	.700879/-02	.440000/-02
.139283/-02	.527337/-02	.700667/-02	.429581/-02
.147898/-02	.533646/-02	.700269/-02	.418986/-02
.156496/-02	.539871/-02	.699682/-02	.408216/-02
.165077/-02	.546010/-02	.698906/-02	.397276/-02
.173640/-02	.552062/-02	.697937/-02	.386170/-02
.182183/-02	.558025/-02	.696775/-02	.374900/-02
.190705/-02	.563896/-02	.695418/-02	.363471/-02
.199206/-02	.569674/-02	.693863/-02	.351888/-02
.207684/-02	.575357/-02	.692110/-02	.340153/-02
.216138/-02	.580944/-02	.690157/-02	.328272/-02
.224568/-02	.586431/-02	.688002/-02	.316249/-02
.232971/-02	.591818/-02	.685643/-02	.304089/-02
.241347/-02	.597102/-02	.683080/-02	.291796/-02
.249695/-02	.602280/-02	.680311/-02	.279375/-02
.258014/-02	.607352/-02	.677335/-02	.266831/-02
.266303/-02	.612316/-02	.674151/-02	.254169/-02
.274560/-02	.617168/-02	.670757/-02	.241395/-02
.282784/-02	.621907/-02	.667153/-02	.228513/-02
.290974/-02	.626531/-02	.663337/-02	.215529/-02
.299129/-02	.631037/-02	.659310/-02	.202448/-02
.307248/-02	.635424/-02	.655069/-02	.189277/-02
.315330/-02	.639690/-02	.650615/-02	.176020/-02
.323372/-02	.643832/-02	.645946/-02	.162683/-02
.331375/-02	.647848/-02	.641063/-02	.149273/-02
.339336/-02	.651736/-02	.635965/-02	.135795/-02
.347255/-02	.655494/-02	.630652/-02	.122255/-02
.355131/-02	.659120/-02	.625123/-02	.108659/-02
.362961/-02	.662611/-02	.619379/-02	.950135/-03
.370744/-02	.665965/-02	.613420/-02	.813240/-03
.378480/-02	.669180/-02	.607245/-02	.675969/-03
.386167/-02	.672254/-02	.600856/-02	.538385/-03
.393804/-02	.675184/-02	.594252/-02	.400550/-03
.401388/-02	.677969/-02	.587434/-02	.262526/-03
.408919/-02	.680606/-02	.580404/-02	.124376/-03
.416396/-02	.683093/-02	.573160/-02	-.138372/-04
-.522938/-03	.542995/-02	.441831/-02	
.545507/-02	-.963063/-01		

APPENDIX 3

Equations (12a), (12b), (13a) (13b) give expressions for G_x and G_y for two extreme cases. Numerical values for G_x and G_y are given in the following tables. These values have been used in Figs. 5, 6 and 7.

$\frac{\rho U h}{\eta}$	$\left\{\left(\frac{\partial p}{\partial x}\right)^2+\left(\frac{\partial p}{\partial y}\right)^2\right\}^{\frac{1}{2}}$	
G_x	G_y	$\frac{\partial p}{\partial x} \ll \frac{\partial p}{\partial y}$
G_x	G_y	$\frac{\partial p}{\partial x} \gg \frac{\partial p}{\partial y}$

.100000/ 04	-.100000/ 04	
.821550/-01	-.139331/ 00	
.819514/-01	.143686/ 00	
.100000/ 04	-.100000/ 05	
.719925/-01	-.857035/-01	
.799911/-01	.105016/ 00	
.100000/ 04	-.500000/ 05	
.439937/-01	-.463187/-01	
.449532/-01	.486339/-01	
.100000/ 04	-.100000/ 06	
.333262/-01	.336596/-01	
.337393/-01	.342968/-01	
.100000/ 04	-.500000/ 06	
.170097/-01	.170514/-01	
.170440/-01	.170880/-01	
.100000/ 04	-.100000/ 07	
.126610/-01	.126757/-01	
.126726/-01	.126874/-01	
.200000/ 04	-.100000/ 04	
.487060/-01	.849737/-01	
.486912/-01	.852222/-01	
.200000/ 04	-.100000/ 05	
.487503/-01	.726759/-01	
.490704/-01	.872996/-01	
.200000/ 04	-.500000/ 05	
.399660/-01	.459749/-01	
.423221/-01	.486654/-01	
.200000/ 04	-.100000/ 06	
.314551/-01	.333963/-01	
.328879/-01	.352002/-01	
.200000/ 04	-.500000/ 06	
.168437/-01	.170159/-01	
.169777/-01	.171548/-01	
.200000/ 04	-.100000/ 07	
.126045/-01	.126811/-01	
.126503/-01	.127097/-01	
.300000/ 04	-.100000/ 04	
.359245/-01	.628206/-01	
.359217/-01	.628853/-01	
.300000/ 04	-.100000/ 05	
.361096/-01	.595050/-01	
.359864/-01	.632077/-01	
.300000/ 04	-.500000/ 05	
.334052/-01	.418970/-01	
.372558/-01	.577506/-01	
.300000/ 04	-.100000/ 06	
.288743/-01	.326487/-01	
.313935/-01	.369652/-01	
.300000/ 04	-.500000/ 06	
.165761/-01	.169536/-01	
.168666/-01	.172886/-01	
.300000/ 04	-.100000/ 07	
.125118/-01	.126420/-01	
.126132/-01	.127472/-01	
.400000/ 04	-.100000/ 04	
.289508/-01	.506500/-01	
.289500/-01	.506631/-01	
.400000/ 04	-.100000/ 05	
.290257/-01	.495433/-01	
.289688/-01	.507625/-01	
.400000/ 04	-.500000/ 05	
.284804/-01	.391168/-01	
.294980/-01	.538928/-01	
.400000/ 04	-.100000/ 06	
.280745/-01	.316540/-01	
.290964/-01	.402879/-01	
.400000/ 04	-.500000/ 06	
.162193/-01	-.168670/-01	
.167092/-01	.174335/-01	
.400000/ 04	-.100000/ 07	
.123848/-01	.126127/-01	
.125809/-01	.128006/-01	
.500000/ 04	-.100000/ 04	
.244889/-01	-.428502/-01	
.244886/-01	.428553/-01	
.500000/ 04	-.100000/ 05	
.245234/-01	.424016/-01	
.244959/-01	.428937/-01	
.500000/ 04	-.500000/ 05	
.245164/-01	.365094/-01	
.246036/-01	.439234/-01	
.500000/ 04	-.100000/ 06	
.233098/-01	.304627/-01	
.255381/-01	.489340/-01	
.500000/ 04	-.500000/ 06	
.157888/-01	.167569/-01	
.165037/-01	.175555/-01	
.500000/ 04	-.100000/ 07	
.122264/-01	.125751/-01	
.124532/-01	.128706/-01	

$\frac{\rho U h}{\eta}$	$\left\{\left(\frac{\partial p}{\partial x}\right)^2+\left(\frac{\partial p}{\partial y}\right)^2\right\}^{\frac{1}{2}}$	
G_x	G_y	$\frac{\partial p}{\partial x} \ll \frac{\partial p}{\partial y}$
G_x	G_y	$\frac{\partial p}{\partial x} \gg \frac{\partial p}{\partial y}$

.600000/ 05	-.100000/ 04	
.206107/-02	.535687/-02	
.206107/-02	.535687/-02	
.600000/ 05	-.100000/ 05	
.206107/-02	.535687/-02	
.206107/-02	.535687/-02	
.600000/ 05	-.500000/ 05	
.206108/-02	.535678/-02	
.206107/-02	.535688/-02	
.600000/ 05	-.100000/ 06	
.206110/-02	.535651/-02	
.206107/-02	.535690/-02	
.600000/ 05	-.500000/ 06	
.206179/-02	.534792/-02	
.206121/-02	.535761/-02	
.600000/ 05	-.100000/ 07	
.206383/-02	.532174/-02	
.206165/-02	.535982/-02	
.900000/ 05	-.100000/ 04	
.280226/-02	.490396/-02	
.280220/-02	.490396/-02	
.900000/ 05	-.100000/ 05	
.280226/-02	.490396/-02	
.280226/-02	.490396/-02	
.900000/ 05	-.500000/ 05	
.280227/-02	.490390/-02	
.280226/-02	.490396/-02	
.900000/ 05	-.100000/ 06	
.280228/-02	.490374/-02	
.280226/-02	.490398/-02	
.900000/ 05	-.500000/ 06	
.280270/-02	.489852/-02	
.280235/-02	.490440/-02	
.900000/ 05	-.100000/ 07	
.280397/-02	.488248/-02	
.280260/-02	.490574/-02	
.100000/ 06	-.100000/ 04	
.258935/-02	.453136/-02	
.258936/-02	.453136/-02	
.100000/ 06	-.100000/ 05	
.258935/-02	.453136/-02	
.258935/-02	.453136/-02	
.100000/ 06	-.500000/ 05	
.258935/-02	.453133/-02	
.258935/-02	.453136/-02	
.100000/ 06	-.100000/ 06	
.258936/-02	.453122/-02	
.258935/-02	.453137/-02	
.100000/ 06	-.500000/ 06	
.258963/-02	.452788/-02	
.258940/-02	.453164/-02	
.100000/ 06	-.100000/ 07	
.259046/-02	.451757/-02	
.258957/-02	.453250/-02	

.200000/ 03	-.500000/ 05	
.456987/-01	-.457841/-01	
.457500/-01	.458156/-01	
.300000/ 03	-.500000/ 05	
.455942/-01	.457407/-01	
.457090/-01	.458567/-01	
.400000/ 03	-.500000/ 05	
.454489/-01	.457000/-01	
.456515/-01	.459148/-01	
.500000/ 03	-.500000/ 05	
.452839/-01	.456660/-01	
.455774/-01	.459895/-01	
.600000/ 03	-.500000/ 05	
.450403/-01	.456148/-01	
.454866/-01	.460817/-01	
.700000/ 03	-.500000/ 05	
.447797/-01	.455544/-01	
.453789/-01	.461946/-01	
.800000/ 03	-.500000/ 05	
.444838/-01	.454849/-01	
.452543/-01	.463199/-01	
.900000/ 03	-.500000/ 05	
.441544/-01	.454063/-01	
.451125/-01	.464670/-01	
.100000/ 04	-.500000/ 05	
.437937/-01	.453187/-01	
.449532/-01	.486339/-01	
.110000/ 04	-.500000/ 05	
.434036/-01	.452223/-01	
.447762/-01	.488212/-01	
.120000/ 04	-.500000/ 05	
.429870/-01	.451171/-01	
.445813/-01	.490301/-01	
.130000/ 04	-.500000/ 05	
.425456/-01	.450032/-01	
.443680/-01	.492617/-01	
.140000/ 04	-.500000/ 05	
.420820/-01	.448808/-01	
.441360/-01	.495174/-01	
.150000/ 04	-.500000/ 05	
.415986/-01	.447500/-01	
.438848/-01	.497986/-01	
.160000/ 04	-.500000/ 05	
.410978/-01	.446109/-01	
.436139/-01	.501073/-01	

$\frac{\rho U h}{\eta}$	$\left\{\left(\frac{\partial p}{\partial x}\right)^2+\left(\frac{\partial p}{\partial y}\right)^2\right\}^{1/2}$	
G_x	G_y	$\frac{\partial p}{\partial x} \ll \frac{\partial p}{\partial y}$
G_x	G_y	$\frac{\partial p}{\partial x} \gg \frac{\partial p}{\partial y}$
.100000/ 04	-.100000/ 04	
.821550/-01	-.139331/ 00	
.819514/-01	.143658/ 00	
.100000/ 04	-.100000/ 05	
.719925/-01	-.857035/-01	
.799911/-01	.105016/ 00	
.100000/ 04	-.500000/ 05	
.437937/-01	-.453187/-01	
.449532/-01	.466339/-01	
.100000/ 04	-.100000/ 06	
.333262/-01	-.338596/-01	
.337393/-01	.342968/-01	
.100000/ 04	-.500000/ 06	
.170097/-01	-.170534/-01	
.170440/-01	.170880/-01	
.100000/ 04	-.100000/ 07	
.126610/-01	-.126757/-01	
.126726/-01	.126874/-01	
.200000/ 04	-.100000/ 04	
.487060/-01	.849737/-01	
.486912/-01	.852222/-01	
.200000/ 04	-.100000/ 05	
.487503/-01	.726759/-01	
.490704/-01	.872996/-01	
.200000/ 04	-.500000/ 05	
.389660/-01	.439749/-01	
.423221/-01	.496634/-01	
.200000/ 04	-.100000/ 06	
.314551/-01	.333963/-01	
.328879/-01	.352002/-01	
.200000/ 04	-.500000/ 06	
.168437/-01	.170159/-01	
.169777/-01	.171548/-01	
.200000/ 04	-.100000/ 07	
.126045/-01	.126631/-01	
.126503/-01	.127097/-01	
.300000/ 04	-.100000/ 04	
.359245/-01	.628206/-01	
.359217/-01	.628653/-01	
.300000/ 04	-.100000/ 05	
.361096/-01	.595050/-01	
.359864/-01	.632077/-01	
.300000/ 04	-.500000/ 05	
.334052/-01	.418970/-01	
.372558/-01	.577506/-01	
.300000/ 04	-.100000/ 06	
.288743/-01	.326487/-01	
.313935/-01	.369652/-01	
.300000/ 04	-.500000/ 06	
.165761/-01	-.169536/-01	
.168666/-01	.172686/-01	
.300000/ 04	-.100000/ 07	
.125118/-01	.126420/-01	
.126132/-01	.127472/-01	
.400000/ 04	-.100000/ 04	
.289508/-01	.506500/-01	
.289500/-01	.506631/-01	
.400000/ 04	-.100000/ 05	
.290257/-01	-.495433/-01	
.289688/-01	.507625/-01	
.400000/ 04	-.500000/ 05	
.284604/-01	-.393168/-01	
.294988/-01	.538928/-01	
.400000/ 04	-.100000/ 06	
.260745/-01	.316540/-01	
.290964/-01	.402879/-01	
.400000/ 04	-.500000/ 06	
.162193/-01	-.160670/-01	
.167092/-01	.174335/-01	
.400000/ 04	-.100000/ 07	
.123848/-01	.126127/-01	
.125609/-01	.128006/-01	
.500000/ 04	-.100000/ 04	
.244889/-01	-.428502/-01	
.244886/-01	.428553/-01	
.500000/ 04	-.100000/ 05	
.245234/-01	-.424016/-01	
.244959/-01	.428937/-01	
.500000/ 04	-.500000/ 05	
.245164/-01	-.365094/-01	
.246836/-01	.439234/-01	
.500000/ 04	-.100000/ 06	
.233998/-01	.304627/-01	
.255381/-01	.489340/-01	
.500000/ 04	-.500000/ 06	
.157888/-01	-.167565/-01	
.165037/-01	.176555/-01	
.500000/ 04	-.100000/ 07	
.122264/-01	.125751/-01	
.124932/-01	.128706/-01	

$\frac{\rho U h}{\eta}$	$\left\{\left(\frac{\partial p}{\partial x}\right)^2+\left(\frac{\partial p}{\partial y}\right)^2\right\}^{1/2}$	
G_x	G_y	$\frac{\partial p}{\partial x} \ll \frac{\partial p}{\partial y}$
G_x	G_y	$\frac{\partial p}{\partial x} \gg \frac{\partial p}{\partial y}$
.600000/ 04	-.100000/ 04	
.213590/-01	-.373757/-01	
.213588/-01	.373781/-01	
.600000/ 04	-.100000/ 05	
.213756/-01	-.371650/-01	
.213622/-01	.373957/-01	
.600000/ 04	-.500000/ 05	
.214793/-01	-.337217/-01	
.214460/-01	.378456/-01	
.600000/ 04	-.100000/ 06	
.210218/-01	-.291354/-01	
.217485/-01	.396591/-01	
.600000/ 04	-.500000/ 06	
.153013/-01	-.166240/-01	
.162474/-01	.179441/-01	
.600000/ 04	-.100000/ 07	
.120398/-01	-.125294/-01	
.124098/-01	.129584/-01	
.700000/ 04	-.100000/ 04	
.190269/-01	-.332959/-01	
.190269/-01	.332971/-01	
.700000/ 04	-.100000/ 05	
.190358/-01	.331854/-01	
.190286/-01	.333062/-01	
.700000/ 04	-.500000/ 05	
.191360/-01	-.311195/-01	
.190716/-01	.335346/-01	
.700000/ 04	-.100000/ 06	
.189879/-01	-.277356/-01	
.192164/-01	.343479/-01	
.700000/ 04	-.500000/ 06	
.147739/-01	-.164693/-01	
.159367/-01	.183128/-01	
.700000/ 04	-.100000/ 07	
.118285/-01	-.124758/-01	
.123101/-01	.130656/-01	
.800000/ 04	-.100000/ 04	
.172137/-01	.301233/-01	
.172137/-01	.301239/-01	
.800000/ 04	-.100000/ 05	
.172180/-01	.300603/-01	
.172146/-01	.301291/-01	
.800000/ 04	-.500000/ 05	
.172951/-01	-.287800/-01	
.172388/-01	.302571/-01	
.800000/ 04	-.100000/ 06	
.172787/-01	-.263218/-01	
.175179/-01	.306892/-01	
.800000/ 04	-.500000/ 06	
.142223/-01	-.162942/-01	
.155666/-01	.187826/-01	
.800000/ 04	-.100000/ 07	
.115964/-01	-.124144/-01	
.121937/-01	.131939/-01	
.900000/ 04	-.100000/ 04	
.157583/-01	-.275766/-01	
.157583/-01	.275770/-01	
.900000/ 04	-.100000/ 05	
.157614/-01	-.275383/-01	
.157589/-01	.275801/-01	
.900000/ 04	-.500000/ 05	
.158160/-01	-.267173/-01	
.157735/-01	.276572/-01	
.900000/ 04	-.100000/ 06	
.158483/-01	-.249413/-01	
.158205/-01	.279103/-01	
.900000/ 04	-.500000/ 06	
.136606/-01	-.160999/-01	
.151299/-01	.193864/-01	
.900000/ 04	-.100000/ 07	
.113474/-01	-.123455/-01	
.120598/-01	.133462/-01	
.100000/ 05	-.100000/ 04	
.145610/-01	-.254815/-01	
.145610/-01	.254817/-01	
.100000/ 05	-.100000/ 05	
.145630/-01	-.254570/-01	
.145614/-01	.254837/-01	
.100000/ 05	-.500000/ 05	
.146016/-01	-.249128/-01	
.145707/-01	.255328/-01	
.100000/ 05	-.100000/ 06	
.146468/-01	-.236268/-01	
.146004/-01	.256914/-01	
.100000/ 05	-.500000/ 06	
.131004/-01	-.158882/-01	
.146165/-01	.201810/-01	
.100000/ 05	-.100000/ 07	
.110852/-01	-.122693/-01	
.119075/-01	.135256/-01	

$\frac{\rho U h}{\eta}$	$\left\{\left(\frac{\partial p}{\partial x}\right)^2+\left(\frac{\partial p}{\partial y}\right)^2\right\}^{1/2}$	
G_x	G_y	$\frac{\partial p}{\partial x} \ll \frac{\partial p}{\partial y}$
G_x	G_y	$\frac{\partial p}{\partial x} \gg \frac{\partial p}{\partial y}$
.110000/ 05	-.100000/ 04	
.135565/-01	-.237236/-01	
.135565/-01	.237238/-01	
.110000/ 05	-.100000/ 05	
.135578/-01	-.237073/-01	
.135567/-01	.237251/-01	
.110000/ 05	-.500000/ 05	
.135852/-01	-.233354/-01	
.135629/-01	.237578/-01	
.110000/ 05	-.100000/ 06	
.136293/-01	-.223973/-01	
.135826/-01	.238622/-01	
.110000/ 05	-.500000/ 06	
.125508/-01	-.156606/-01	
.140102/-01	.212774/-01	
.110000/ 05	-.100000/ 07	
.108136/-01	-.121861/-01	
.117358/-01	.137367/-01	
.120000/ 05	-.100000/ 04	
.127000/-01	.222249/-01	
.127000/-01	.222251/-01	
.120000/ 05	-.100000/ 05	
.127010/-01	.222136/-01	
.127002/-01	.222260/-01	
.120000/ 05	-.500000/ 05	
.127208/-01	-.219524/-01	
.127045/-01	.222485/-01	
.120000/ 05	-.100000/ 06	
.127590/-01	.212608/-01	
.127180/-01	.223201/-01	
.120000/ 05	-.500000/ 06	
.120189/-01	-.154192/-01	
.132817/-01	.229650/-01	
.120000/ 05	-.100000/ 07	
.105358/-01	.120961/-01	
.115432/-01	.139854/-01	
.130000/ 05	-.100000/ 04	
.119601/-01	-.209300/-01	
.119601/-01	.209301/-01	
.130000/ 05	-.100000/ 05	
.119607/-01	.209220/-01	
.119602/-01	.209308/-01	
.130000/ 05	-.500000/ 05	
.119752/-01	-.207339/-01	
.119632/-01	.209468/-01	
.130000/ 05	-.100000/ 06	
.120069/-01	-.202177/-01	
.119728/-01	.209974/-01	
.130000/ 05	-.500000/ 06	
.115095/-01	-.151657/-01	
.123817/-01	.238716/-01	
.130000/ 05	-.100000/ 07	
.102550/-01	-.119998/-01	
.113281/-01	.142799/-01	
.140000/ 05	-.100000/ 04	
.113134/-01	-.197985/-01	
.113134/-01	.197985/-01	
.140000/ 05	-.100000/ 05	
.113139/-01	-.197926/-01	
.113135/-01	.197990/-01	
.140000/ 05	-.500000/ 05	
.113247/-01	-.196541/-01	
.113157/-01	.198107/-01	
.140000/ 05	-.100000/ 06	
.113504/-01	-.192639/-01	
.113227/-01	.198475/-01	
.140000/ 05	-.500000/ 06	
.110257/-01	-.149024/-01	
.115941/-01	.215305/-01	
.140000/ 05	-.100000/ 07	
.997385/-02	-.118974/-01	
.110885/-01	.146321/-01	
.150000/ 05	-.100000/ 04	
.107429/-01	-.188001/-01	
.107429/-01	.188001/-01	
.150000/ 05	-.100000/ 05	
.107433/-01	-.187957/-01	
.107430/-01	.188005/-01	
.150000/ 05	-.500000/ 05	
.107515/-01	.186918/-01	
.107446/-01	.188092/-01	
.150000/ 05	-.100000/ 06	
.107721/-01	-.183926/-01	
.107498/-01	.188366/-01	
.150000/ 05	-.500000/ 06	
.105691/-01	-.146311/-01	
.109417/-01	.199657/-01	
.150000/ 05	-.100000/ 07	
.969461/-02	-.117894/-01	
.108208/-01	.150598/-01	

$\frac{\rho U h}{\eta}$	$\left\{\left(\frac{\partial p}{\partial x}\right)^2+\left(\frac{\partial p}{\partial y}\right)^2\right\}^{1/2}$	
G_x	G_y	$\frac{\partial p}{\partial x} \ll \frac{\partial p}{\partial y}$
G_x	G_y	$\frac{\partial p}{\partial x} \gg \frac{\partial p}{\partial y}$
.160000/ 05	-.100000/ 04	
.102353/-01	-.179117/-01	
.102355/-01	.179118/-01	
.160000/ 05	-.100000/ 05	
.102356/-01	-.179084/-01	
.102354/-01	.179120/-01	
.160000/ 05	-.500000/ 05	
.102419/-01	-.178291/-01	
.102366/-01	.179187/-01	
.160000/ 05	-.100000/ 06	
.102584/-01	-.175972/-01	
.102406/-01	.179394/-01	
.160000/ 05	-.500000/ 06	
.101403/-01	-.143540/-01	
.103814/-01	.187436/-01	
.160000/ 05	-.100000/ 07	
.941927/-02	-.116761/-01	
.105215/-01	.155921/-01	
.170000/ 05	-.100000/ 04	
.978034/-02	.171156/-01	
.978034/-02	.171156/-01	
.170000/ 05	-.100000/ 05	
.978055/-02	-.171130/-01	
.978038/-02	.171158/-01	
.170000/ 05	-.500000/ 05	
.978546/-02	.170515/-01	
.978135/-02	.171209/-01	
.170000/ 05	-.100000/ 06	
.979881/-02	.168694/-01	
.978440/-02	.171369/-01	
.170000/ 05	-.500000/ 06	
.973896/-02	.140731/-01	
.989060/-02	.177317/-01	
.170000/ 05	-.100000/ 07	
.914942/-02	-.115580/-01	
.101845/-01	.162027/-01	
.180000/ 05	-.100000/ 04	
.936993/-02	-.163973/-01	
.936992/-02	.163974/-01	
.180000/ 05	-.100000/ 05	
.937009/-02	-.163953/-01	
.936996/-02	.163975/-01	
.180000/ 05	-.500000/ 05	
.937397/-02	-.163469/-01	
.937072/-02	.164015/-01	
.180000/ 05	-.100000/ 06	
.938478/-02	-.162024/-01	
.937311/-02	.164141/-01	
.180000/ 05	-.500000/ 06	
.934434/-02	-.137900/-01	
.945494/-02	.168662/-01	
.180000/ 05	-.100000/ 07	
.888633/-02	-.114355/-01	
.979959/-02	.172581/-01	
.190000/ 05	-.100000/ 04	
.899757/-02	-.157457/-01	
.899757/-02	.157458/-01	
.190000/ 05	-.100000/ 05	
.899770/-02	-.157441/-01	
.899760/-02	.157459/-01	
.190000/ 05	-.500000/ 05	
.900080/-02	-.157056/-01	
.899820/-02	.157491/-01	
.190000/ 05	-.100000/ 06	
.900961/-02	-.155896/-01	
.900010/-02	.157590/-01	
.190000/ 05	-.500000/ 06	
.901515/-02	-.135067/-01	
.906428/-02	.161100/-01	
.190000/ 05	-.100000/ 07	
.863098/-02	-.113091/-01	
.934477/-02	.183391/-01	
.200000/ 05	-.100000/ 04	
.865801/-02	-.151515/-01	
.865800/-02	.151515/-01	
.200000/ 05	-.100000/ 05	
.865811/-02	-.151502/-01	
.865803/-02	.151516/-01	
.200000/ 05	-.500000/ 05	
.866062/-02	.151192/-01	
.865852/-02	.151542/-01	
.200000/ 05	-.100000/ 06	
.866784/-02	.150252/-01	
.866004/-02	.151622/-01	
.200000/ 05	-.500000/ 06	
.868992/-02	.132246/-01	
.871112/-02	.154395/-01	
.200000/ 05	-.100000/ 07	
.838408/-02	.111791/-01	
.891511/-02	.168170/-01	

$\frac{\rho U h}{\eta}$	$\left\{\left(\frac{\partial p}{\partial x}\right)^2+\left(\frac{\partial p}{\partial y}\right)^2\right\}^{1/2}$	
G_x	G_y	$\frac{\partial p}{\partial x} \ll \frac{\partial p}{\partial y}$
G_x	G_y	$\frac{\partial p}{\partial x} \gg \frac{\partial p}{\partial y}$
.300000/ 05	-.100000/ 04	
.638777/-02	-.111786/-01	
.638778/-02	.111786/-01	
.300000/ 05	-.100000/ 05	
.638779/-02	-.111784/-01	
.638778/-02	.111786/-01	
.300000/ 05	-.500000/ 05	
.638825/-02	-.111728/-01	
.638786/-02	.111791/-01	
.300000/ 05	-.100000/ 06	
.638964/-02	-.111555/-01	
.638814/-02	.111805/-01	
.300000/ 05	-.500000/ 06	
.641764/-02	-.106887/-01	
.639692/-02	.112270/-01	
.300000/ 05	-.100000/ 07	
.641293/-02	.978656/-02	
.642564/-02	.113837/-01	
.400000/ 05	-.100000/ 04	
.514808/-02	-.900914/-02	
.514809/-02	.900914/-02	
.400000/ 05	-.100000/ 05	
.514809/-02	-.900908/-02	
.514808/-02	.900915/-02	
.400000/ 05	-.500000/ 05	
.514822/-02	-.900743/-02	
.514811/-02	.900928/-02	
.400000/ 05	-.100000/ 06	
.514864/-02	-.900231/-02	
.514819/-02	.900970/-02	
.400000/ 05	-.500000/ 06	
.515984/-02	-.884915/-02	
.515076/-02	.902329/-02	
.400000/ 05	-.100000/ 07	
.517665/-02	-.846884/-02	
.515891/-02	.906661/-02	
.500000/ 05	-.100000/ 04	
.435475/-02	-.762081/-02	
.435472/-02	.762081/-02	
.500000/ 05	-.100000/ 05	
.435475/-02	-.762078/-02	
.435475/-02	.762081/-02	
.500000/ 05	-.500000/ 05	
.435480/-02	-.762014/-02	
.435476/-02	.762086/-02	
.500000/ 05	-.100000/ 06	
.435496/-02	-.761816/-02	
.435479/-02	.762103/-02	
.500000/ 05	-.500000/ 06	
.435975/-02	-.755654/-02	
.435578/-02	.762624/-02	
.500000/ 05	-.100000/ 07	
.437058/-02	-.738541/-02	
.435891/-02	.764275/-02	
.600000/ 05	-.100000/ 04	
.379819/-02	-.664684/-02	
.379818/-02	.664684/-02	
.600000/ 05	-.100000/ 05	
.379819/-02	-.664683/-02	
.379819/-02	.664684/-02	
.600000/ 05	-.500000/ 05	
.379822/-02	-.664653/-02	
.379820/-02	.664686/-02	
.600000/ 05	-.100000/ 06	
.379829/-02	-.664562/-02	
.379821/-02	.664694/-02	
.600000/ 05	-.500000/ 06	
.380059/-02	-.661678/-02	
.379867/-02	.664934/-02	
.600000/ 05	-.100000/ 07	
.380663/-02	-.653237/-02	
.380010/-02	.665689/-02	
.700000/ 05	-.100000/ 04	
.338351/-02	-.592114/-02	
.338353/-02	.592114/-02	
.700000/ 05	-.100000/ 05	
.338351/-02	-.592113/-02	
.338351/-02	.592114/-02	
.700000/ 05	-.500000/ 05	
.338352/-02	-.592098/-02	
.338351/-02	.592115/-02	
.700000/ 05	-.100000/ 06	
.338356/-02	-.592050/-02	
.338352/-02	.592119/-02	
.700000/ 05	-.500000/ 06	
.338477/-02	-.590541/-02	
.338375/-02	.592243/-02	
.700000/ 05	-.100000/ 07	
.338820/-02	-.586006/-02	
.338450/-02	.592634/-02	

$\frac{\rho U h}{\eta}$	$\left\{\left(\frac{\partial p}{\partial x}\right)^2+\left(\frac{\partial p}{\partial y}\right)^2\right\}^{1/2}$	
G_x	G_y	$\frac{\partial p}{\partial x} \ll \frac{\partial p}{\partial y}$
G_x	G_y	$\frac{\partial p}{\partial x} \gg \frac{\partial p}{\partial y}$
.800000/ 05	-.100000/ 04	
.306107/-02	-.535687/-02	
.306107/-02	.535687/-02	
.800000/ 05	-.100000/ 05	
.306107/-02	-.535687/-02	
.306107/-02	.535687/-02	
.800000/ 05	-.500000/ 05	
.306108/-02	-.535678/-02	
.306107/-02	.535688/-02	
.800000/ 05	-.100000/ 06	
.306110/-02	.535651/-02	
.306107/-02	.535690/-02	
.800000/ 05	-.500000/ 06	
.306179/-02	.534792/-02	
.306121/-02	.535761/-02	
.800000/ 05	-.100000/ 07	
.306383/-02	-.532174/-02	
.306163/-02	.535982/-02	
.900000/ 05	-.100000/ 04	
.280226/-02	.490396/-02	
.280220/-02	.490396/-02	
.900000/ 05	-.100000/ 05	
.280226/-02	-.490396/-02	
.280226/-02	.490396/-02	
.900000/ 05	-.500000/ 05	
.280227/-02	-.490390/-02	
.280226/-02	.490396/-02	
.900000/ 05	-.100000/ 06	
.280228/-02	-.490374/-02	
.280226/-02	.490398/-02	
.900000/ 05	-.500000/ 06	
.280270/-02	-.489852/-02	
.280235/-02	.490440/-02	
.900000/ 05	-.100000/ 07	
.280397/-02	-.488248/-02	
.280260/-02	.490574/-02	
.100000/ 06	-.100000/ 04	
.258935/-02	-.453136/-02	
.258936/-02	.453136/-02	
.100000/ 06	-.100000/ 05	
.258935/-02	-.453136/-02	
.258955/-02	.453136/-02	
.100000/ 06	-.500000/ 05	
.258935/-02	-.453133/-02	
.258935/-02	.453136/-02	
.100000/ 06	-.100000/ 06	
.258936/-02	-.453122/-02	
.258935/-02	.453137/-02	
.100000/ 06	-.500000/ 06	
.258963/-02	-.452788/-02	
.258940/-02	.453164/-02	
.100000/ 06	-.100000/ 07	
.259046/-02	-.451757/-02	
.258957/-02	.453250/-02	

$\frac{\rho U h}{\eta}$	$\left\{\left(\frac{\partial p}{\partial x}\right)^2+\left(\frac{\partial p}{\partial y}\right)^2\right\}^{1/2}$	
G_x	G_y	$\frac{\partial p}{\partial x} \ll \frac{\partial p}{\partial y}$
G_x	G_y	$\frac{\partial p}{\partial x} \gg \frac{\partial p}{\partial y}$
.200000/ 03	-.500000/ 05	
.456987/-01	-.457641/-01	
.457500/-01	.458156/-01	
.300000/ 03	-.500000/ 05	
.455942/-01	.457407/-01	
.457090/-01	.458567/-01	
.400000/ 03	-.500000/ 05	
.454489/-01	.457080/-01	
.456515/-01	.459146/-01	
.500000/ 03	-.500000/ 05	
.452639/-01	.456660/-01	
.455774/-01	.459895/-01	
.600000/ 03	-.500000/ 05	
.450403/-01	.456148/-01	
.454866/-01	.460817/-01	
.700000/ 03	-.500000/ 05	
.447797/-01	-.455544/-01	
.453789/-01	.461916/-01	
.800000/ 03	-.500000/ 05	
.444838/-01	-.454849/-01	
.452543/-01	.463199/-01	
.900000/ 03	-.500000/ 05	
.441544/-01	.454063/-01	
.451125/-01	.464670/-01	
.100000/ 04	-.500000/ 05	
.437937/-01	.453187/-01	
.449532/-01	.466339/-01	
.110000/ 04	-.500000/ 05	
.434038/-01	.452223/-01	
.447762/-01	.468212/-01	
.120000/ 04	-.500000/ 05	
.429870/-01	.451171/-01	
.445813/-01	.470301/-01	
.130000/ 04	-.500000/ 05	
.425456/-01	.450032/-01	
.443680/-01	.472617/-01	
.140000/ 04	-.500000/ 05	
.420820/-01	-.448808/-01	
.441360/-01	.475174/-01	
.150000/ 04	-.500000/ 05	
.415986/-01	.447500/-01	
.438848/-01	.477986/-01	
.160000/ 04	-.500000/ 05	
.410978/-01	-.446109/-01	
.436139/-01	.481073/-01	

STELLINGEN

1. De in dit proefschrift afgeleide vergelijkingen voor drukopbouw en stroming in een smeerfilm zijn niet alleen geldig voor turbulente stroming maar ook voor laminaire.

   (Zie dit proefschrift, vergelijkingen (8a) en (8b), vul in $n_o = 0.066$ en $m_o = -0.25$ voor turbulente stroming en $n_o = 12$ en $m_o = -1$ voor laminaire stroming.)

2. De ongevoeligheid van de vergelijkingen voor het stromingstype doet verwachten dat ze ook in het overgangsgebied tussen laminaire en turbulente stroming geldig zullen zijn.

   Vanzelfsprekend moeten empirische constanten die kenmerkend voor dit overgangsgebied zijn in de vergelijkingen ingevuld worden.

3. In een turbulente smeerfilm met een overheersende sleurstroomcomponent, is de drukstroomcomponent onderworpen aan een richtingsafhankelijke stromingsweerstand die maximaal is wanneer de richtingen van de stromingscomponenten samenvallen en die minimaal is wanneer de richtingen loodrecht op elkaar staan.

   Deze stromingscondities treden op in zelfwerkende lagers en bevorderen de zijlek.

   (Zie dit proefschrift, fig. 5a en b.)

4. Het toepassen van ruwe loopvlakken is een effectieve manier om de invloed van stroomversnellingen en -vertragingen in een turbulente smeerfilm relatief klein te houden.

   (Zie dit proefschrift, formule 10c.)

5. De in dit proefschrift ontwikkelde theorie inspireert tot een eenvoudiger weergave van experimentele resultaten dan de theorie op basis van de wandwet.

   (Zie dit proefschrift, fig. 4.)

6. De proeven van Favre aan een vleugel met een huid, die over de omtrek van het vleugelprofiel glijdt, zijn van groot belang voor de ontwikkeling van vliegtuigen die steil kunnen stijgen en landen.

   (Favre A., Contribution à l'étude experimentale des mouvements hydrodynamiques à deux dimensions, Publ. scientifiques et techniques du Ministère de l'Air, no 137 (1938)).

7. De door Favre ondervonden technische moeilijkheden bij het glijden van de huid om de vleugel zijn te wijten aan:
   - de relatief grote dikte van de huid -
   - de aandrijving en geleiding met rollen van grote lengte -
   - de droge wrijving tussen huid en buitenomtrek van de eigenlijke vleugel -.